ISOTOPIC AND GEOCHEMICAL INVESTIGATION INTO THE ORIGIN OF ELEVATED URANIUM CONCENTRATIONS IN TREASURE VALLEY GROUND AND SURFACE WATERS, IDAHO

by

Brian Hanson

A thesis

submitted in partial fulfillment

of the requirements for the degree of

Master of Science in Hydrologic Sciences

Boise State University

December 2011

© 2011

Brian Hanson

ALL RIGHTS RESERVED

BOISE STATE UNIVERSITY GRADUATE COLLEGE

DEFENSE COMMITTEE AND FINAL READING APPROVALS

of the thesis submitted by

Brian Hanson

Thesis Title: Isotopic and Geochemical Investigation into the Origin of Elevated Uranium Concentrations in Treasure Valley Ground and Surface Waters, Idaho

Date of Final Oral Examination: 26 August 2011

The following individuals read and discussed the thesis submitted by student Brian Hanson, and they evaluated his presentation and response to questions during the final oral examination. They found that the student passed the final oral examination.

Shawn Benner, Ph.D.	Co-Chair, Supervisory Committee
Mark Schmitz, Ph.D.	Co-Chair, Supervisory Committee
James McNamara, Ph.D.	Member, Supervisory Committee

The final reading approval of the thesis was granted by Shawn Benner, Ph.D., and Mark Schmitz, Ph.D., Co-Chairs of the Supervisory Committee. The thesis was approved for the Graduate College by John R. Pelton, Ph.D., Dean of the Graduate College.

ABSTRACT

This study was initiated to evaluate potential source(s) of elevated uranium in ground and surface waters of the Treasure Valley in southwest Idaho. Groundwater in the area exhibits widespread but complexly distributed uranium concentrations up to 110 μg L^{-1}, well in excess of the U.S. EPA drinking water standard of 30 μg L^{-1}. Data from field sampling (surface water, groundwater, and solid sediments), laboratory experiments, and geochemical and isotopic analysis constrain the source of the elevated uranium. Results from surface water sampling show significant downstream increases in uranium concentrations. With irrigation return waters and shallow groundwater returns indicated as the primary contributors toward elevated uranium concentrations, evidence suggests that a near-surface uranium source exists within the valley. When evaluated for isotopic composition, these surface waters consistently evolved toward a common nexus of $^{234}U/^{238}U$ and $^{87}Sr/^{86}Sr$ isotopic composition that is also shared by the estimated mean groundwater composition and several of the most elevated groundwater samples. Analysis of a wide variety of geologic materials representing aquifer sediments did not uncover materials containing particularly high bulk uranium contents (avg. of 3.5 ppm). Furthermore, isotopic analysis of nearly all the solids produced low $^{234}U/^{238}U$ ratios that are incompatible with the source material. In addition, isotopic results definitively indicate that the analyzed fertilizers cannot be the source of the uranium. Only two shallow geologic samples collected from terrace and floodplain sediment yielded high

enough $^{234}U/^{238}U$ ratios to match the projected source signature. Isotopic and elemental differences between three selective leaching treatments applied to each solid show that, on average, the most uranium and highest $^{234}U/^{238}U$ ratios were associated with the carbonate extraction. The two high $^{234}U/^{238}U$ solids did not contain particularly high carbonate contents, and it appears that the carbonate leaching solution acts to assist in releasing the source uranium from sorption and exchange sites in some shallow, fine-grained, clastic sediments of the Gowen Terrace and modern floodplain formations.

TABLE OF CONTENTS

ABSTRACT iv

LIST OF FIGURES ix

LIST OF TABLES xi

1 INTRODUCTION 1

1.1 The Problem 1

1.2 Uranium Release and Control 2

1.3 Uranium and Strontium Isotopic Systematics 4

1.4 Geology/Lithology 7

1.5 Hydrology 8

1.6 Climate 9

1.7 Hydrogeology 10

1.8 Phosphate Fertilizers 11

2 MATERIALS AND METHODS 13

2.1 Existing Data Evaluation 13

2.2 Field Sampling 14

2.2.1 Surface Water Sampling 14

2.2.2 Groundwater Sampling 15

2.2.3 Solid/Sediment Collection 16

2.3 Solid Dissolution and Leaching Experiments 16

2.3.1 Total Dissolutions 17
2.3.2 Selective Extractions 18
2.4 Analytical Methods 20
2.4.1 Anion Analysis 20
2.4.2 Cation Analysis 20
2.4.3 MINTEQ Modeling 21
2.4.4 Isotopic Analysis 21
3 RESULTS 22
3.1 Existing Data Analysis 22
3.2 Surface Water 23
3.2.1 Surface Water Elemental Results 23
3.2.2 Surface Water Isotopic Results 25
3.3 Groundwater 27
3.3.1 Groundwater Elemental Results 27
3.3.2 Groundwater Isotopic Results 28
3.4 Total Solid Dissolutions 29
3.5 Selective Extractions 30
3.5.1 Selective Extraction Elemental Results 30
3.5.2 Selective Extraction Isotopic Results 31
3.6 Phosphate Fertilizer and Ore Analysis 33
4 DISCUSSION 34
4.1 Surface and Groundwaters Influenced by Common Source 34
4.2 Interpretation of Solids Extraction Results 37

4.3 The Role of Carbonates in Uranium Mobility 41

4.4 The Isotopic Incompatibility of Fertilizers 45

4.5 Possible Areas for Further Study 46

5 CONCLUSIONS 47

5.1 Near Surface Uranium Source 47

5.2 Isotopic Similarity in Contaminated Ground and Surface Waters 49

5.3 Phosphate Fertilizer Cannot Be the Uranium Source 50

5.4 Carbonate Dissolution and Carbonate-Assisted Leaching Yield the Highest Uranium Concentrations and Present the Best Isotopic Fit to the Contamination Source 50

REFERENCES 52

APPENDIX A 80

Complete Geochemical Data for Surface Water Samples 80

APPENDIX B 83

Complete Geochemical Data for Groundwater Samples 83

APPENDIX C 85

Complete Geochemical Data for Solid Extraction Experiments 85

LIST OF FIGURES

Figure 1: Surface Water, Groundwater, and Solids Sampling Locations 58

Figure 2: Treasure Valley Groundwater Uranium Distributions from Existing Agency Dataset 59

Figure 3: Plots of U Concentration vs Well Depth and vs Distance from Redox Transition Feature 60

Figure 4: Relationships Between Groundwater U and Other Dissolved Species and Parameters from Existing Agency Dataset 61

Figure 5: Relationships Between Surface Water U and Other Dissolved Species and Parameters 62

Figure 6: Relationships Between Surface Water Sr and Other Dissolved Species and Parameters 63

Figure 7: Surface Water Isotopic Compositions 64

Figure 8: Surface Water U and Sr Isotopic Evolution and Mixing 65

Figure 9: Relationships Between Groundwater U and Other Dissolved Species and Parameters 66

Figure 10: Relationships Between Groundwater Sr and Other Dissolved Species and Parameters 67

Figure 11: Groundwater Isotopic Compositions 68

Figure 12: Groundwater U and Sr Isotopic Evolution and Mixing 69

Figure 13: Solid Extraction Leachable Content Elemental Results 70

Figure 14: Solid Extraction Leachate Isotopic Compositions 72

Figure 15: Average Isotopic Compostions of Solid Extraction Scenarios 73

Figure 16: Relationships Between U Isotopic Composition and Leachable Contents of Several Ions for Samples 1#4 and 7#1 74

LIST OF TABLES

Table 1: Uranium Statistics for Public vs Private Well Data..... 75

Table 2: Surface Water Sample Details 76

Table 3: Groundwater Sample Details 77

Table 4: Total Uranium Content of Solids and Phosphate Samples 78

Table 5: Total Dissolution and Selective Extraction Results..... 79

1 INTRODUCTION

1.1 The Problem

Drinking water contaminated with high uranium is a human health issue and emerging regulatory concern for public drinking water providers since the US Environmental Protection Agency (EPA) establishment of a maximum contaminant level (MCL) standard for uranium at 30 μg L^{-1}. The primary health effects related to excessive uranium consumption are kidney toxicity and increased occurrence of cancer (US EPA, 2009). Typical natural abundances of uranium in groundwater can range from 0.1 to 100 μg L^{-1} (Wanty & Nordstrom, 1995). However, while granitic materials represent one of the more uranium-rich lithologies, groundwater interacting with granitic materials rarely exceed 20 μg L^{-1} (Gascoyne, 1989). Within the Western Snake River Plain (Treasure Valley) Aquifer, dissolved uranium concentrations exceed the 30 μg L^{-1} standard at many locations and concentrations as high as 110 μg L^{-1} have been measured (IDWR, 2010; IDEQ, 2010).

Within the Treasure Valley, a complex sedimentary history is described by the materials that fill the basin. Ancient lake and river sediments comprise the deep aquifer unit, where anthropogenic influences such as the modern onset of irrigation or water level fluctuations tied to deep well withdrawals may stimulate the deep release of uranium. Surficial, vadose zone, and shallow aquifer materials all have the potential to interact with the surface water and shallow aquifer units. Weathering of the wide variety of

fluvial, alluvial, and eolian materials present in these surficial and shallow geologic environments may also be implicated for elevated uranium observed in Treasure Valley groundwater. Phosphate fertilizers, a politically contentious uranium source, are often high in uranium and their utilization for agricultural purposes may be an important contamination source.

The goal of this thesis is to constrain the source of uranium to Treasure Valley groundwater and surface waters. I propose the hypothesis that a specific unit of near-surface sediments is releasing uranium, but that the source sediments are not ubiquitously distributed throughout the region. As an alternative hypothesis, I suggest that uranium-rich fertilizers may be an important uranium contamination source to the Treasure Valley hydrologic system. To test these hypotheses, a multi-faceted approach was employed whereby the analysis of surface water, groundwater, and solid extraction samples were all used to provide evidence for or against each potential source. Surface waters were most valuable in investigating dissolved uranium dynamics in the most surficial units. Groundwater samples were interpreted as interacting with both the surficial and shallow geologic environments and were thus helpful in investigating the degree of connectedness between surface and groundwater sources. Finally, total dissolutions and selective extractions of solid phase materials were ultimately used to test for the uranium content and isotopic character of a wide variety of potential source solids.

1.2 Uranium Release and Control

The behavior of uranium in groundwater is determined by a complex interplay of chemical and physical conditions. The concentration of dissolved uranium in a given system can be a function of that environment's redox status, concentrations of

complexing agents, presence of sorption sites, as well as hydrologic interaction with uranium source materials (McKinley et al., 2007; Elless & Lee, 1998). Uranium typically exists in natural waters in its U (VI) oxidation state as a uranyl oxycation [UO_2^{2+} or UO_2OH^+]. In these states, uranium is highly soluble and acts conservatively in aqueous solution. Under reducing conditions, U (IV) is the dominant oxidation state. The low solubility of U(IV) under reducing conditions leads to precipitation of minerals such as uraninite, coffinite.

The uranyl ion commonly forms strong aqueous complexes with carbonate [i.e. $UO_2(CO_3)_x$, $Ca_xUO_2(CO_3)_x$] in most groundwaters; these complexes can dramatically increase effective solubility and total dissolved concentrations (Langmuir, 1997; Clark et al., 1995; Pabalan & Turner, 1997; Elless & Lee, 1998). When dissolved carbonate contents are particularly low, or the concentrations of other ligands are abnormally high, uranium may also complex with other electron donor groups, such as: hydroxide [$UO_2(OH)_x$], sulfate [UO_2SO_4], fluoride [UO_2F_2], etc. (Buck et al., 1996; Langmuir, 1997). These latter complexes are still relatively soluble, but cannot compete with carbonate's ability to complex uranium under neutral or alkaline pH conditions. At low pH conditions, the uranyl sulfate complex or the solitary uranyl cation may dominate. In the rare absence of the previously mentioned complexing agents or the presence of very high concentrations of silicates, phosphates, or arsenates, less soluble uranium complexes can form, but will more readily be precipitated out of solution (McKinley et al., 2007; Smith, 1984).

Dissolved uranium is also known to be susceptible to sorption onto negatively charged metal oxide and aluminosilicate mineral surfaces. These sorption reactions can

compete with the previously mentioned complexing agents (such as carbonate and sulfate) and retard uranium mobility (McKinley et al., 2007; Prikryl et al., 2001).

1.3 Uranium and Strontium Isotopic Systematics

As $^{234}U/^{238}U$ and $^{87}Sr/^{86}Sr$ isotopic ratio analysis is a central component of this investigation, a brief discussion of each isotope system is valuable. Uranium occurs naturally in the form of three different isotopes (with decreasing nuclide stability): ^{238}U, ^{235}U, and ^{234}U. Because ^{238}U and ^{234}U are part of the same decay series, they are closely associated to each another, with ^{234}U being a relatively short-lived (halflife = 2.45×10^5 years) daughter product of radiogenic ^{238}U (halflife = 4.47×10^9 years) decay. Therefore, their abundances are also related. The ^{238}U isotope comprises more than 99% of the natural abundance of uranium (Steiger & Jäger, 1977), while ^{234}U accounts for less than .01% (Lide & Frederikse, 1995). Due to the relative scarcity of ^{234}U, a quotient of $^{234}U/^{238}U$ will always yield a very small number. For this reason, the ratio of ^{234}U to ^{238}U will sometimes be converted to an activity ratio by multiplying the abundances of ^{234}U and ^{238}U by their respective decay constants. Activity ratios conveniently express the same relationship in larger numbers. Additionally, the use of activity ratios provides a convenient baseline value equal to 1.0 for ^{234}U and ^{238}U at a state of secular equilibrium (Faure & Mensing, 2005).

Secular equilibrium is the terminal $^{234}U/^{238}U$ ratio that a given geologic sample will asymptotically evolve toward subsequent to any isotopic fractionation. For the $^{234}U/^{238}U$ system, it can generally be assumed that a given rock will closely approach secular equilibrium after several ^{234}U half-lives worth of time have passed since its formation. Therefore, the majority of crustal materials (rocks older than approx. 1-2

million years) have $^{234}U/^{238}U$ activity ratios of approximately 1.0 (Luo et al., 2000). However, groundwater $^{234}U/^{238}U$ ratios typically exceed the secular equilibrium value (Roback et al., 2001). The disequilibrium between waters and the solids with which they interact can be traced back to the alpha recoil events caused by ^{238}U decay. The high energy alpha recoil events damage the crystal matrix surrounding the product ^{234}U atoms, leaving ^{234}U susceptible to be preferentially leached relative to ^{238}U (Grzymko et al., 2007). Additionally, alpha recoil can cause ^{234}U (via ^{234}Th) to be directly ejected from the solid matrix into solution or onto adjacent surfaces (Roback et al., 2001; Osmond et al., 1968; Maher et al., 2006). Interpretation of the $^{234}U/^{238}U$ ratios in waters at disequilibrium with the solids they weather can provide a variety of insights into the nature of the solids and the dynamics of the water-solid interaction.

The $^{87}Sr/^{86}Sr$ isotopic system is fundamentally different to that of $^{234}U/^{238}U$ in that ^{87}Sr and ^{86}Sr do not share a parent-daughter relationship. Strontium naturally occurs in the form of four stable isotopes: ^{88}Sr, ^{87}Sr, ^{86}Sr, and ^{84}Sr. The only radiogenic isotope is ^{87}Sr, which is created by the decay of ^{87}Rb. While strontium is an alkaline earth metal that can largely substitute for calcium in a mineral matrix, rubidium is an alkali metal that can substitute in potassium-bearing minerals. Therefore, the $^{87}Sr/^{86}Sr$ ratio of a solid, for example, can be greatly influenced by the mineralogical contents of the solid. Generally speaking, $^{87}Sr/^{86}Sr$ ratios can be used as a sort of barometer between mafic and felsic mineral compositions (Faure & Mensing, 2005). More specifically, potassium and rubidium-rich minerals (e.g. K-feldspars; K-rich phyllosilicates) will have the opportunity to develop relatively higher $^{87}Sr/^{86}Sr$ ratios through the growth of radiogenic

^{87}Sr, compared to minerals that tend to exclude potassium and have higher calcium and strontium contents (carbonates, plagioclase feldspars).

In hydrologic investigations, isotopic ratios can be used as high precision tracers of the source(s) of masses of water, and can provide information about the weathering history of the watershed. The use of isotopic ratios as tracers provides unique benefits not available when using ion concentrations alone. Processes such as sorption and precipitation may prevent ion concentrations from being considered as conservative tracers, but these processes do not affect isotopic ratios. The use of $^{234}U/^{238}U$ ratios alone have proven useful in estimating sources of groundwater recharge (Roback et al., 2001), discovering preferential groundwater flow paths (Luo et al., 2000), calculating mixing proportions of multiple source waters (Osmond et al., 1968; Grzymko et al., 2007), and studying the rates and dynamics of water-rock interaction (Andersen et al., 2009; Maher et al., 2004). The $^{87}Sr/^{86}Sr$ system has been used similarly (Johnson et al., 2000; Jeon & Nakano, 2001; Johnson & DePaolo, 1994), with the added intricacy that the $^{87}Sr/^{86}Sr$ system may be especially targeted towards identifying sources of calcium weathering products (Clow et al., 1997). The coupling together of uranium and strontium isotopic systems in hydrologic investigations provides for unique, high precision, two-component descriptions of the isotopic signature of waters and the solids that they interact with (Maher et al., 2006; Chabaux et al., 2005; Riotte & Chabaux, 1999). Additionally, the concurrent use of the two isotopic systems allows for interpretations based on the observation of contrasting behavior between $^{234}U/^{238}U$ and $^{87}Sr/^{86}Sr$ ratios. Uranium isotopic behavior differs from that of strontium as $^{234}U/^{238}U$ disequilibrium caused by alpha recoil effects and selective leaching of ^{234}U is a property exclusive to the uranium

isotopic system. Conversely, the ability of $^{87}Sr/^{86}Sr$ ratios to differentiate between mafic and felsic sources makes the strontium isotopic system unique in its own right.

1.4 Geology/Lithology

The Treasure Valley Aquifer is hosted in sedimentary fill of a Neogene aged, normal fault-bounded intracontinental rift basin that defines the Western Snake River Plain (Wood & Clemens, 2002). The approximately 300 km long by 70 km wide, southeast to northwest trending basin is bordered on the southwest by the rhyolitic Owyhee Front, and to the northeast by the Idaho Batholith-derived Boise Front. Below approximately 2000 meters of fill, the basin is underlain by basalt. The complex sedimentary history of the Western Snake River Plain includes repeated episodes of ancient lake formation and draining, fluvial and alluvial deposition, as well as loess and ash deposition (Wood & Clemens, 2002). The deepest aquifer units are housed within one to two thousand meters of monotonous mudstones composed of ancient lacustrine sediments of the Chalk Hills and Glenns Ferry formations. Sitting unconformably atop of the massive mudstones are an additional 60 to 90 meters of interbedded sands, silts, and mudstones of the Glenns Ferry and Pierce Park formations (Wood & Clemens, 2002). The shallow aquifer is composed of diverse fluvial sediments and gravels of the Boise and Snake Rivers as well as alluvium from side-stream valleys. These poorly-sorted deposits form a series of abandoned river terraces ranging up to approximately 24 meters in thickness. The terrace dominated topography is such that the oldest terraces (including the Gowen Terrace) are located near the center of the basin, with progressively younger terraces descending in elevation towards the locations of the modern Boise and Snake River floodplains. Ash and loess materials are interspersed throughout the basin fill and a

mantle of up to 3 meters of loess accumulations top most terrace materials (Othberg & Stanford, 1992). The surficial soils are generally carbonate-rich, often exhibiting a distinct calcic horizon at 30-100 cm depth.

Many well drillers' logs from throughout the basin demonstrate a distinct zone of sediment color from brown/orange above to gray/blue below. The transition generally occurs below the shallow river terrace sediments, at depths ranging between 2 and 130 meters. The transition is not clearly associated with a specific lithologic unit, but has been interpreted as a remnant of the historic water table, prior to the modern onset of irrigation (Busbee et al., 2009). As the sediment color change near the transition is indicative of the redox status of the sediments, the redox transition has largely been considered to be a boundary between deep lake sediments (reducing) and shallower fluvial and alluvial sediments (oxidizing) (Petrich & Urban, 2004; Hutchings & Petrich, 2002). As is the case with many elements, uranium's aqueous mobility is dependent on redox conditions. For this reason, the sediment redox transition zone may be important in studying the presence of uranium in aquifer solids.

1.5 Hydrology

The Treasure Valley's hydrology is strongly influenced by the Boise River, which flows along the northwest side of the Treasure Valley before reaching its confluence with the Snake River. While water from the Snake River may influence the deepest aquifer units, Boise River water is the dominant source of recharge to the aquifer, primarily through an extensive network of irrigation canals that have been conveying water toward both Lake Lowell Reservoir and flood irrigated lands in the center and western reaches of the valley since the late 1800's (Petrich & Urban, 2004). While the Boise River receives

the vast majority of its waters from the upper portion of the watershed in the central Idaho mountains, smaller volumes of water also enter the valley by way of tributaries emanating from the nearby Boise Front, canals importing Payette River water at the northeastern portion of the valley, irrigation return waters from within the Treasure Valley, and direct precipitation (Cosgrove & Taylor, 2007; Thoma et al., 2011).

Several other regional rivers were considered in this study, not necessarily because they are hydrologically connected to the Treasure Valley, but because they were considered to represent diverse geologies present in the region. These regional rivers include the previously mentioned Snake and Payette Rivers, as well as the Owyhee and Weiser Rivers. These rivers are characteristic of some of the diverse geologies present throughout the region. The Owyhee River represents a predominantly rhyolitic watershed; the Weiser River, a basaltic watershed; the Payette River, a primarily granitic watershed, and the Snake River, an expansive and complex watershed that is largely of sedimentary character.

1.6 Climate

The Treasure Valley is located in the semi-arid west, a climate marked by low to moderate annual precipitation relative to the evapotranspiration rate. Average annual precipitation is approximately 28 cm while evapotranspiration (prior to irrigation) is estimated to be approximately 27 cm (Urban, 2004). Temperatures average 23°C in the summer and -2°C in the winter (Petrich & Urban, 2004). With annual evapotranspiration nearly equaling precipitation at the valley floor, very little groundwater recharge can be credited to direct infiltration of valley precipitation under pre-irrigation conditions.

1.7 Hydrogeology

The aquifer system underlying the Treasure Valley has been previously well characterized (Hutchings & Petrich, 2002; Petrich & Urban, 2004; Squires & Wood, 2001; Urban, 2004; Wood & Clemens, 2002). In summary, the greater aquifer is generally described as a stratigraphically complex environment comprising a series of sedimentary aquifer units ranging from shallow units composed of coarse-grained, unconsolidated sediments, down to the finer grained units and monotonous mudstones of the deep aquifer. These aquifer units are conceptually divided into a deep regional aquifer and a shallow local aquifer system. Although there is some hydrologic interaction between the two systems, a transitional boundary of fine-grained materials largely confines the deep aquifer and provides for two distinct flow regimes (Petrich & Urban, 2004).

The deep aquifer is as much as several thousand meters thick in parts of the basin. It receives recharge from losing reaches of the Boise River and from regional underflow conveyed from adjacent basins north and east of the Treasure Valley. Deep aquifer flows are generally westward as they discharge to gaining reaches of the Boise and Snake Rivers. The deep aquifer system is generally, but not uniformly, segregated from the overlaying strata of interbedded sands, gravels, and silts that house the shallow aquifer units. The deep regional aquifer exhibits confined or semi-confined characteristics at many well locations (Cosgrove & Taylor, 2007).

The shallow aquifer is as much as 200 meters thick in central parts of the basin. The shallow aquifer contains many water-bearing zones interspersed with less permeable sediments. Stratification within the shallow aquifer is thought to significantly limit

vertical communication between the various water-bearing zones (Hutchings & Petrich, 2002). Recharge to the shallow system comes from local sources, and is dominated by infiltration of applied irrigation water and seepage from the irrigation canal network (Petrich & Urban, 2004). Throughout most of the Treasure Valley, irrigation water is primarily composed of Boise River water. Additional recharge comes from precipitation and losses from the Boise River channel. Annual infiltration from the irrigation related sources is estimated to be approximately 146 cm yr^{-1}, compared to about 1 cm yr^{-1} from precipitation alone (Urban, 2004). The significantly higher recharge rate related to the onset of modern irrigation has increased the average water table elevation relative to historic conditions. As the increase in water table elevation is greatest where irrigation is most concentrated, water table mounding occurs within central and western portions of the valley. The groundwater divide created by this mound influences groundwater flow direction in the shallow aquifer such that flows travel generally northwest prior to the divide before veering either north toward the Boise River or west toward the Snake River (Petrich & Urban, 2004).

1.8 Phosphate Fertilizers

As trace uranium contents in phosphate ore rocks have the potential to be particularly enriched in comparison to crustal averages (Zielinski et al., 1997, 2000; Taylor, 2007), phosphate fertilizers must be considered as a potential anthropogenic uranium contamination source. Phosphate fertilizers commonly used by Treasure Valley agricultural operations (such as ammonium phosphate) are typically produced through the mining and processing of ore rock formations (such as the Phosphoria formation in Eastern Idaho). High uranium contents found in these phosphate ore rocks are conveyed

to the fertilizer products and potentially to the environments where the fertilizers are used. The distinct $^{234}U/^{238}U$ isotopic composition of phosphate fertilizers can be used to evaluate the potential contributions of fertilizer-derived uranium to the environment (Zielinski et al., 2006).

2 MATERIALS AND METHODS

Due to the high cost of extracting an extensive collection of *in situ* aquifer sediment core samples for this investigation, an approach was adapted to study Treasure Valley uranium dynamics and evaluate the source hypotheses from several different angles. This multi-faceted approach was employed to use the analysis of surface water, groundwater, and solid extraction samples in providing multiple pieces of evidence either support or rejecting each source hypothesis. Surface waters were most valuable in investigating dissolved uranium dynamics in the more surficial units. Groundwater samples were interpreted as interacting with both the surficial and shallow geologic environments and were thus helpful in investigating the degree of connectedness between surface and groundwater sources. Finally, total dissolutions and selective extractions of solid phase materials were ultimately used to test for the uranium content and isotopic character of a wide variety of solids in search, in search of materials releasing uranium isotopically congruent with the dissolved uranium observed in ground and surface waters.

2.1 Existing Data Evaluation

Existing groundwater geochemical data was collected from the Idaho Department of Water Resources' Statewide Groundwater Quality Monitoring Network (IDWR, 2010) and from the Idaho Department of Environmental Quality's Public Water System Database (IDEQ, 2010). The combined dataset was limited to data-points representing wells within the Treasure Valley study area that were previously analyzed for dissolved

uranium concentration. A total of more than 160 unique, private and public well locations were compiled to evaluate existing agency data. Additionally, well depth and construction information for the wells were investigated by accessing the IDWR online Well Log Database. The existing well location and uranium concentration data was imported into an ArcGIS database to create an aerial-view geospatial representation of where regions of high and low uranium concentration exist within the Treasure Valley. All other geochemical data (cations, anions, pH, alkalinity, etc.) were used to observe broad trends between the occurrence of uranium and other geochemical parameters. Well depths were combined with uranium concentration data to plot and examine the spatial relationships between uranium concentration and depth below ground surface, depth below water table, and distance to aquifer sediment redoximorphic transition. The ArcGIS data layers necessary to estimate the locations of the water table and redoximorphic transition were previously constructed for a different groundwater investigation within the same study area (Busbee et al., 2009).

2.2 Field Sampling

2.2.1 Surface Water Sampling

A total of 30 surface water samples were collected over three sampling events (Figure 1). Each sampling event was timed to represent one of two temporally distinct periods: late-summer irrigation season, or mid-winter dormant season. Sample collection was centered around the Lower Boise River (the reach below Lucky Peak Dam), as this water is the primary input to the underlying Treasure Valley Aquifer. Several Boise River tributaries were sampled to capture contributions from various catchments and irrigation

return systems. Additionally, four other regional rivers were sampled to investigate the influence of diverse catchment geologies on the geochemical character of their surface waters.

All water samples were collected into plastic bottles that had been cleaned with high purity HNO_3. Prior to bottling, samples were passed through 0.45 µm (micron) filters. Samples for cation and isotopic analysis were immediately acidified to pH 2.0 with high purity HNO_3. Samples for anion analysis were filtered but not acidified. All sample bottles were stored at 4°C until analysis. Simultaneous to sample collection, pH, specific conductance, and dissolved oxygen, oxidative/reductive potential were determined using a YSI field meter. Alkalinity was determined in the field by titration (HACH), and a field chemistry kit was also used to confirm dissolved oxygen values.

2.2.2 Groundwater Sampling

A total of eight groundwater well samples were collected from a combination of wells serving either public water systems or private households (Figure 1). Wells sampled were chosen based upon their location and the results of previous uranium concentration analysis, as informed by the existing agency data. Eight distributed well samples were not considered to be enough to spatially cover the study area. Therefore, the sampling strategy focused on first sampling from wells that were suspected of yielding high uranium concentrations, then seeking to find a nearby well with a significantly contrasting uranium concentration signal.

Groundwater sampling required the construction of a split hose device. This device was used to convey water from the source well into a groundwater flow cell chamber with the YSI field meter installed within it. This setup allowed for the

continuous observation of field measurement parameters as a means of deciding when the well had been sufficiently purged of water before collecting a sample volume that was representative of the aquifer and not containing excessive artifacts of the well construction materials. Once the well was deemed to have been sufficiently purged, the flow could split such that sample filtration and collection could occur while maintaining flow through the flow cell. All other details of sample collection, preservation, and storage were conducted in accordance with the description from the preceding section.

2.2.3 Solid/Sediment Collection

A total of 22 solid samples were collected for total dissolution and selective leaching experiments (Figure 1). Six outcropping/exposure sample locations were chosen to best capture a representative array of the complex assortment of geologic formations that contribute materials to the Treasure Valley Aquifer. The technical assistance of Dr. Spencer Wood (a locally experienced field geologist) was used in accurately identifying outcroppings of older sediment units. Additionally, one recently extracted well core from the Boise State University campus was obtained for sampling of in situ shallow aquifer solids. At each location, between one and five samples were collected along the stratigraphic profile. Solid samples were sealed and stored in plastic bags prior to being oven dried in preparation for analysis.

2.3 Solid Dissolution and Leaching Experiments

Solid samples were subjected to four distinct dissolution treatments designed to target different fractions of the solid matrix. While the solid fraction extracted by each

dissolution treatment is ultimately operationally defined, the goals for each treatment were as follows.

The total dissolution procedure was intended to completely dissolve the solid matrix, thereby producing a solution indicative of the total chemical composition of the solid material. The deionized water (DI) extraction was intended to leach only the most easily released, water soluble fraction. The acetic acid extraction was intended to dissolve carbonate materials, liberate exchangeable ions, and also leach the water soluble fraction. The hydroxylamine extraction was intended to dissolve the reducible Fe oxide fraction, while also being aggressive enough to incorporate the species released by the DI water and acetic acid treatments.

2.3.1 Total Dissolutions

In order to achieve total dissolution of the solids, a lithium tetra-borate fusion method was applied to a portion of each the solid samples. The method was a modified version of those found in literature (Jarvis et al., 1992). Samples were ground to a fine powder in a SPEX CertiPrep Shatterbox using an alumina ceramic container. The ceramic container was cleaned and pre-contaminated before and after processing each sample. Approximately 250 mg of the powdered sample was then mixed with 500 mg of lithium tetra-borate flux, transferred to a clean graphite crucible, and placed in a 900°C muffle furnace for at least 30 minutes to ensure complete melting of the sample. The resulting glass bead was weighed and transferred to a clean 500 ml HDPE bottle, and dissolved and diluted to 500 grams gravimetrically using 2% HNO_3, with 300 μl concentrated HF and 1 ml concentrated H_2O_2 added to assist in dissolving silicate and organic materials respectively. The solution was left overnight on a shaker table to fully

dissolve, resulting in a solution with a dilution factor of 2000x that is further diluted 2x online during analysis (4000x total dilution).

2.3.2 Selective Extractions

The three selective extraction methods (DI water, acetic acid, and hydroxylamine) were developed by comparing and modifying extraction and leaching procedures represented in the literature (Schultz et al., 1998; Blanco et al., 2005; Dhoum & Evans, 1998; La Force & Fendorf, 2000; Martin et al., 1998; Tessier et al., 1979; Thomas et al., 1994). Each extraction technique was performed on a fresh portion of solid sample and the procedures were conducted parallel to one another, rather than in a series. Most combinations of sample and extraction technique were performed in sets of three replicates in order to account for the natural variability of the solid materials. In cases of limited original solid sample, two replicates were used. Each extraction was performed within a 50 ml Teflon FEP (Oakridge) centrifuge tube using 1.0 g of dried solid that had been homogenized and sieved to < 2 mm.

The DI water extraction was designed to leach only the water soluble ions from the solids. For this extraction, 30 ml of 18 MΩ deionized H_2O was added to the solid samples. With the centrifuge tubes sealed, the slurries were constantly perturbed 20 hours using an automatic shaker set at 120 rpm. After shaking, the slurries were centrifuged at 3500 rpm for 45 min and the supernate solution was decanted, filtered to 0.45 microns, and acidified to < 1% HNO_3.

The acetic acid extraction was designed to leach carbonate bound and exchangeable ions out of the solids. The extractant was composed of 1.0 M NaAc/HAc buffered to pH 4.5. A 20 ml volume of extractant was added to the solid samples and the

slurries were shaken for 2 hrs. After centrifuging and decanting the supernate solution, a fresh 20 ml volume of extractant was added to the solids and a second series of shaking and decanting was performed. The additional shaking treatment was included to assure that the carbonate dissolving capacity of the extractant was not neutralized by alkaline soils. The two batches of resulting supernate solutions were combined and filtered to 0.45 microns.

The hydroxylamine extraction was designed to leach reducible Fe, Mn, and Al oxide-associated ions out of the solids. The extractant was composed of 0.1 M NH_2OH-HCl brought to pH 2.0 with the addition of HNO_3. A 30 ml volume of extractant was added to the solid samples and the slurries were shaken for 5 hrs. The sample were centrifuged, decanted, and filtered as described above.

An aliquot of each selective extraction solution was analyzed for its elemental composition, and the remaining solution was reserved for uranium and strontium isotopic analysis. Based on the results of the chemical analysis, some of the extraction samples were deemed to be inappropriate for isotopic analysis. Many of the DI water extractions were too dilute for proper isotopic analysis. These dilute samples were re-extracted using a higher solid sample masses specifically for isotopic analysis. Due to an apparent strontium contamination issue traced to the NaAc reagent, most of the acetic acid extractions were also unsuitable for isotopic analysis. A set of acetic acid extractions were repeated for isotopic analysis purposes using 0.5 M HAc without the addition of NaAc.

2.4 Analytical Methods

2.4.1 Anion Analysis

Anion analysis utilized a Lachat brand ion chromatography (IC) unit with a carbonate eluent solution and sulfuric acid regenerant. In order to prevent excessive degradation of several anionic compounds, all water samples were analyzed within 48 hours of their collection. The specific procedure for anion analysis was based on EPA method #300.0. The measure of instrument precision for the IC was determined by conducting duplicate analyses of several samples. Instrument accuracy was determined by conducting frequent calibration standard checks throughout each IC run. Instrument precision typically exceeded accuracy. In several cases, the samples used to measure precision contained extremely low concentrations of a given anion; this caused poorer than normal precision values for those anions. IC precision, accuracy, blank, and detection limit values can be seen in Appendices A, B, and C.

2.4.2 Cation Analysis

Cation analysis was accomplished by utilizing a Thermo Electron X Series 2 quadruple inductively coupled plasma mass spectrometer (ICP-MS) with a high purity argon gas carrier and high purity 2% nitric acid as the sample solution matrix. ICP-MS analysis was conducted with a procedure based on EPA method #200.8. ICP-MS precision was evaluated by observing the standard deviations between the multiple “sweeps” employed by the instrument on every sample. This measure of precision is generally high and exceeds the instrument accuracy in most cases. Some cations, which are almost always present in the samples at minute concentrations, will yield precision

measures that are poorer than the instrument accuracy measure. ICP-MS accuracy was evaluated by conducting frequent calibration standard checks throughout each analysis run. As an additional inspection of data quality, both anion and cation results were input into MINTEQ geochemical modeling software to obtain charge balances for each sample. ICP-MS precision, accuracy, blank, detection limit, and charge balance values can be seen in Appendices A, B, and C.

2.4.3 MINTEQ Modeling

Aqueous geochemical modeling software, Visual MINTEQ, was used to assess the chemical speciation and complexation of all groundwater and select surface water samples. The software also allowed for charge balance analysis, an additional data quality check. Charge balance analysis reinforced the quality of the cation and anion data, showing that all samples exhibited charge differences of approximately 8% or less (Appendix B).

2.4.4 Isotopic Analysis

$^{234}U/^{238}U$ and $^{87}Sr/^{86}Sr$ isotopic ratios were measured by using a multi-collector Thermal Ionization Mass Spectrometry (TIMS) instrument. TIMS analysis was conducted in accordance with established Boise State University Isotope Geology Lab procedures which are representative of methods used in current literature (Schmitz & Bowring, 2001). Uncertainty associated with the uranium and strontium isotopic ratio data was determined by observing the 1 σ variability within each run. For $^{234}U/^{238}U$ ratios, uncertainty is < 1% for all samples. For $^{87}Sr/^{86}Sr$ ratios, uncertainty is < .001% for all samples.

3 RESULTS

3.1 Existing Data Analysis

Growing concern over the occurrence of elevated uranium in the Treasure Valley Aquifer represents emerging regulatory attention to the contamination issue. Prior to the 2003 establishment of an EPA drinking water standard for uranium, there was no requirement for direct measurement of dissolved uranium. Therefore, the quantity of publically available surface and groundwater uranium data is more sparse than for other contaminants.

The groundwater data accumulated for this study, by joining public and private well datasets, likely represents the most extensive dataset of uranium occurrence in the Treasure Valley created to date. Among the more than 100 well locations that represent public water systems, the mean uranium concentration was found to be 18 $\mu g\ L^{-1}$ (median of 12 $\mu g\ L^{-1}$) and the high value was 95 $\mu g\ L^{-1}$. Among the more than 60 private well locations with uranium data, the mean concentration was 33 $\mu g\ L^{-1}$ (median of 26 $\mu g\ L^{-1}$) and the high value was 110 $\mu g\ L^{-1}$ (Table 1). This survey indicates that groundwater exceeding the EPA standard of 30 $\mu g\ L^{-1}$ is present throughout the region (Figure 2). However, there is no consistent pattern in the aerial distribution of high uranium concentrations. Instead, several uranium hot-spots exist. Additionally, the existing agency data do not show any clear relationship between uranium concentration and depth or distance from the interpolated redox transition zone (Figure 3).

Plots of uranium concentration vs concentrations of other elements and parameters revealed few correlations (Figure 4). One trend that does stand out is the relationship between alkalinity ($CaCO_3$) and the potential for high uranium concentrations. That is to say that high alkalinity samples could be associated with either high or low uranium concentrations, while low alkalinity samples are consistently associated with low uranium. The highest uranium concentrations are also associated with slightly alkaline pH and moderate specific conductance values.

3.2 Surface Water

Unlike groundwater data, no previous Treasure Valley surface water uranium data is known to exist. For this reason, surface water sampling was conducted both within the lower Boise River watershed, as well as at other regional rivers.

3.2.1 Surface Water Elemental Results

Several observations can be made from the surface water sampling results. On the Boise River, repeated seasonal sampling occurred at three locations reaching from the most upstream location, just below Lucky Peak Dam, to the most downstream location, just before the confluence with the Snake River (Figure 1). Boise River uranium concentrations undergo an approximate 18-fold increase along this reach (Table 2). During summer/irrigation season, uranium concentrations increased upstream to downstream from 0.3 to 5.6 $\mu g\ L^{-1}$. Winter/dormant season concentrations increased from 0.6 to 9.9 $\mu g\ L^{-1}$.

Inputs to the river that may be contributing significant loads of uranium include: tributaries draining the foothills region to the north of the river, tributaries from the south

of the river containing agricultural irrigation return flows, and shallow groundwater flows discharging to the river channel. Dry Creek and Willow Creek, two northern tributaries sampled as they emanate from the foothills, were found to have low uranium concentrations with maximum values of 2.9 and 1.4 μg L^{-1} respectively. Indian Creek and 10 Mile Creek, two southern tributaries draining agricultural land, were found to have uranium concentrations as high as 10.3 and 16.4 μg L^{-1} respectively. In fact, synoptic sampling of Indian and 10 Mile Creeks revealed low uranium concentrations (similar to upstream Boise River water) exist at upstream locations before undergoing a 10 to 20-fold increase near their confluences with the Boise River.

Surface water uranium concentrations within the Boise and Owyhee Rivers as well as Indian and 10 Mile Creeks increase in correlation with a variety of major dissolved cationic and anionic species (Figure 5). Several relationships, especially U vs Sr and U vs Ca, appear to be robust enough that all of the surface waters plot in a well-defined array. Relationships between uranium and alkalinity, specific conductance, and K also show strong positive correlations, although different surface waters appear to be represented by slightly different vectors. There are, however, several species that share weaker correlations with uranium, and U vs Fe appear to be negatively correlated. Plots of Sr vs other species and parameters show that uranium and strontium are well correlated, and that they are behaving similarly in Treasure Valley surface waters (Figure 6). As was the case with uranium, strontium shows reasonably strong positive correlations with many common ions, and negative or no correlation with Fe.

3.2.2 Surface Water Isotopic Results

Another key element of the surface and groundwater analysis is the $^{234}U/^{238}U$ and $^{87}Sr/^{86}Sr$ isotopic ratios of the samples. Independent of the concentrations of uranium and strontium in a given sample, the isotopic composition provides a unique and detailed fingerprint of the sample that can be used to differentiate waters from different sources and to compare high uranium waters to their potential contamination sources.

Surface waters, both within the Treasure Valley and within the broader region, exhibit diverse isotopic compositions, owing primarily to the diverse lithologies of their respective source catchments. The isotopic extremes observed within the study area include upstream Owyhee River and Dry Creek representing the highest and lowest $^{234}U/^{238}U$ values respectively, with Snake and Weiser Rivers representing the highest and lowest $^{87}Sr/^{86}Sr$ values respectively (Figure 7). Surface water isotopic compositions remain fairly consistent between multiple sampling events with relatively minor fluctuations between seasons. Several locations sampled a year apart, but in the same season (IC#2, 10C#2, and OR#3), yielded almost identical isotopic compositions.

The isotopic compositions of the Boise River, Indian Creek, and 10 Mile Creek all begin at their upstream sampling locations exhibiting different isotopic compositions, primarily marked by moderate $^{234}U/^{238}U$ and high $^{87}Sr/^{86}Sr$ values. As uranium concentrations increase downstream, their isotopic compositions evolve toward a higher $^{234}U/^{238}U$ and lower $^{87}Sr/^{86}Sr$ isotopic region. Additionally, the Owyhee River, a regional river draining a separate watershed, begins with very high $^{234}U/^{238}U$ but moderate $^{87}Sr/^{86}Sr$ values before abruptly evolving toward the common isotopic composition also exhibited by the previously mentioned downstream surface waters of the Boise River's

watershed. This common region of isotopic space toward which multiple surface waters evolve is referred to as the nexus of convergence.

Plots of uranium (and strontium) isotopic compositions vs reciprocal uranium (and strontium) concentrations show the isotopic evolution of the surface waters as they become more concentrated in uranium and (strontium). These plots provide the necessary transformation to investigate the linearity of two-component mixtures (Riotte & Chabaux, 1999; Roback et al., 2001). Boise River, 10-Mile Creek, and Indian Creek all experience increasing $^{234}U/^{238}U$ ratios corresponding to dissolved uranium increases (Figure 8). Boise River and 10-Mile Creek isotopic compositions trend toward near equivalent $^{234}U/^{238}U$ values, while Indian Creek and Owyhee River compositions also trend toward similar, but slightly higher $^{234}U/^{238}U$ values. In terms of strontium isotopic evolution, Boise River, 10-Mile Creek, and Indian Creek all consistently decrease in $^{87}Sr/^{86}Sr$ as strontium concentrations increase (Figure 8). Again the compositions of Boise River and 10-Mile Creek waters evolve toward nearly equivalent $^{87}Sr/^{86}Sr$ compositions while Indian Creek evolves toward a similar but slightly lower $^{87}Sr/^{86}Sr$ value. With respect to both uranium and Strontium isotopic evolution, Boise River, 10-Mile Creek, and Indian Creek waters all show similar dynamics in that they are all evolving toward a common range of isotopic compositions and each mixing line shows predominantly two component mixing.

3.3 Groundwater

3.3.1 Groundwater Elemental Results

Among the eight groundwater wells sampled (Figure 1), three yielded uranium concentrations exceeding the EPA standard of 30 μg L^{-1}. Each of these three samples contained >50 μg L^{-1} uranium, with the most heavily contaminated sample having approximately 74 μg L^{-1} dissolved uranium (Table 3). The comparison between uranium concentrations and depths for wells sampled in this study shows a trend of highest uranium occurring at the shallowest depths, a trend that was not demonstrated in the existing dataset (Figure 3).

Uranium concentrations show positive correlations with a number of other dissolved species and parameters (Figure 9). The strongest linear correlations exist between uranium and alkalinity, nickel, strontium, and perhaps iron. While numerous correlations exist between uranium and other dissolved species in surface waters, uranium in groundwater samples shows fewer relationships. As groundwater uranium does not correlate well with specific conductance, high uranium concentrations do not appear to simply be a function of high total dissolved solids. Additionally, several plots appear to show bifurcating relationships between uranium and other parameters (especially conductivity and potassium, but potentially others as well) where the data points split into two separate vectors instead of grouping into a single array. With a limited number of points in the dataset, it is difficult to determine if these trends are anything more than typical data scatter.

Modeling of groundwater geochemistry using MINTEQ software showed that uranium's occurrence in groundwater is consistently dominated by the $Ca_2UO_2(CO_3)_{3(aq)}$ (approx. 65%) and $CaUO_2(CO_3)_3^{-2}$ (approx. 34%) complexes, with significantly smaller concentrations of $UO_2(CO_3)_3^{-4}$ (approx. 1%) and other uranyl carbonates. Most samples were at or near saturation conditions with carbonate minerals such as calcite, aragonite, or dolomite. Saturation with a variety of silicate mineral was also common.

Strontium concentrations are positively correlated with uranium; therefore, strontium shares most of the same correlations seen between uranium and other species and parameters (Figure 10). Strontium has an especially strong linear correlation with calcium, but also exhibits a somewhat weaker relationship with alkalinity than does uranium. As with the previously seen in the uranium data, bifurcations also appear in the data plots of strontium vs conductivity and potassium. These trends are similar but slightly less obvious than those seen in the uranium data. Again, a larger sample population would be needed to elucidate the potential importance of these bifurcations.

3.3.2 Groundwater Isotopic Results

The isotopic compositions of the groundwater well samples collected for this study show more diversity than downstream Treasure Valley surface waters, but still form a distinct cluster when compared to the diffuse spread of regional surface water compositions (Figure 11). Treasure Valley groundwater samples are identified by moderate to high $^{234}U/^{238}U$ and moderate $^{87}Sr/^{86}Sr$ values. Most of the well samples plot within, or at a close proximity to, the contamination source nexus previously proposed for surface waters. The wells nearest to the nexus are the most clearly affected by the uranium source influencing the surface waters. Those wells that plot further from the

nexus are likely affected by separate (but similar) sources, or a mixture of sources. Additionally, it should be noted that among the eight well samples, the three with the highest uranium concentrations (> 50 μg L^{-1}) all plot in the same low $^{234}U/^{238}U$ and high $^{87}Sr/^{86}Sr$ corner of the groundwater isotopic cluster.

Uranium isotopic composition vs reciprocal concentration plots show that the groundwater samples with highest uranium contents (lowest 1/U values) have relatively little spread in $^{234}U/^{238}U$ ratios compared to samples with moderate and low uranium contents (Figure 12). The overall spread in uranium isotopic compositions is indicative of multiple isotopicaly diverse end-members being expressed in low to moderate uranium concentration samples, but converging toward the lower $^{234}U/^{238}U$ ratios represented in high uranium groundwater samples. By contrast, strontium isotopic composition vs reciprocal concentration plots show a clear trend of low strontium (high 1/Sr) samples being associated with lower $^{87}Sr/^{86}Sr$ ratios and higher strontium samples consistently evolving toward higher $^{87}Sr/^{86}Sr$ values (Figure 12). The strength of this trend, although not perfectly linear, suggests a predominantly two component mixing scenario with distinctly different dynamics than that of the groundwater uranium isotopic system. Although groundwater uranium and strontium concentrations were found to be reasonably well correlated, the differences in their respective mixing scenarios would seem to indicate that the two elements are not consistently being released in a coupled process.

3.4 Total Solid Dissolutions

The complete dissolution of solids served to investigate whether Treasure Valley aquifer sediments contain unusually high uranium contents, and what range of variability

exists between the different materials. Among the wide variety of lithologies collected, none of the solids were remarkably uraniferious (Table 4). The average total uranium content of the solids was approximately 3.5 ppm, and ranged from 0.9 to 7.0 ppm. Lithologies representing the Treasure Valley aquifer are generally consistent with the 2.7 ppm average uranium content for continental crustal materials and with global average granitic materials averaging 4.4 ppm (Wanty and Nordstrom, 1995). Materials from carbonate and iron oxide enriched horizons, as well as several silt samples, were the most uraniferious lithologies. Several coarse sand samples contained the least uranium.

3.5 Selective Extractions

Selective extraction experiments served to address several questions. Among them: Do different solid mineral fractions exhibit the ability yield significantly more uranium than others? Which lithologies and extraction scenarios demonstrate the greatest capacity for uranium leaching? And which Treasure Valley sedimentary formations most closely match the proposed isotopic signature of the uranium source?

3.5.1 Selective Extraction Elemental Results

While overall uranium concentrations for the Treasure Valley sediments are not elevated, the selective extraction experiments indicate that certain fractions of the solids hold more uranium than others (Figure 13). The DI water soluble fraction had the lowest average leachable uranium content at 5.8 ppb. Compared to the 3.5 ppm average total uranium content of solids, the average DI water soluble uranium fraction comprised only about 0.2% of total uranium. However, some lithologies released considerably more uranium. Several samples rich in carbonates (1#2, 2#1, and 4#2) or iron oxides (3#1 and

4#3) released about three times the average amount of uranium, with a maximum value of 16.9 ppb (Table 5). Several silt samples also contained above average DI water soluble uranium contents. Given the elevated DI water leachable uranium in carbonate and iron oxide lithologies, it is no surprise that the two extractions targeted at carbonates and iron oxides produced significantly higher leachable uranium values. Average carbonate and iron oxide leachable uranium contents were 532 ppb and 309 ppb respectively (or about 15% and 9% of total uranium).

The overall highest leachable uranium content for all permutations of lithologies and extractants was 2,740 ppb, and came from sample 1#2, a surficial carbonate enriched horizon subjected to the carbonate targeting extractant. In fact, the carbonate extraction was responsible for the majority of the highest leachable uranium contents (Figure 13). However, not all of these high uranium releasing solids were heavy in carbonate minerals. For most solids, the carbonate extractant released nearly equal or greater uranium than did the oxide extractant. This trend even holds true for the iron oxide-rich solids, where it was expected that only the oxide targeting extractant would release significant uranium.

3.5.2 Selective Extraction Isotopic Results

The isotopic composition of the leachates resulting from each selective extraction ultimately dictates which solids can be potentially implicated as the uranium source(s) in the Treasure Valley. While a wide range of $^{87}Sr/^{86}Sr$ ratios are present in the solids, the majority of samples exhibited low $^{234}U/^{238}U$ isotopic characters (Figure 14). However, two samples (1#4 and 7#1) seem to break the low $^{234}U/^{238}U$ ceiling and plot within the nexus of U-Sr isotopic space toward which multiple Treasure Valley ground and surface

water were found to converge. Sample 1#4 yielded relatively high $^{234}U/^{238}U$ ratios from each of its three extractions, with the carbonate extraction yielding the highest $^{234}U/^{238}U$ value. Only the carbonate extraction produced a high $^{234}U/^{238}U$ ratio from 7#1, with significantly lower $^{234}U/^{238}U$ ratios associated with the other two extractions. These two samples of interest were both fine-grained strata from shallow alluvial formations. Sample 1#4 was found within the Gowen Terrace formation, and sample 7#1 came from a well core extracted out of the modern floodplain. Interestingly, other nearby sediments of differing lithologies within the Gowen Terrace and modern floodplain formations exhibit lower $^{234}U/^{238}U$ ratios.

Different extractions scenarios applied to the same solid sample most often resulted in similar leachate isotopic characteristics, with the three extractions plotting in clusters. For samples that exhibited greater spread between their extractants, the carbonate (acetic acid) extraction typically yielded the highest $^{234}U/^{238}U$ value. In fact, the overall average isotopic compositions for each extraction scenario show that the carbonate extraction yields the highest $^{234}U/^{238}U$ ratios, with the DI water extraction yielding the lowest values (Figure 15).

Investigations seeking to isolate any specific elemental concentrations that increase in correlation with leachate $^{234}U/^{238}U$ ratios between the three extraction scenarios uncovered few useful trends that held true for all (or even most) of the wide lithologic variety of solid samples. However, considering only the two samples of greatest interest (1#4 and 7#1), a positive correlation between leachable potassium content and $^{234}U/^{238}U$ ratios can be seen (Figure 16). Sample 1#4 alone also shows a trend between $^{234}U/^{238}U$ and arsenic, and possibly with strontium as well.

3.6 Phosphate Fertilizer and Ore Analysis

Compared to the total uranium contents from all of the geologic solids collected and to the published estimates, crustal averages, phosphate fertilizers, and the types of ore rocks that they are produced from were found to be quite uraniferious (Table 4), and the fertilizers have been implicated as a potential anthropogenic uranium contamination source (Zielinski et al., 1997, 2000, 2006; Taylor, 2007). The most uranium-laden of three commercial fertilizer products contained 319 ppm uranium. At 38 ppm, the lowest uranium fertilizer sample was still significantly more uraniferious than any of the solids representing Treasure Valley aquifer materials. Analysis of phosphate ore rocks from a one Phosphoria Formation source suggests that there may be little or no reduction of uranium content in the process of creating phosphate fertilizer from ore deposits. The isotopic compositions of the fertilizer products approximately matched those of the total dissolutions of ore rocks (Figure 14). However, both phosphate fertilizer and ore rocks consistently showed very low $^{234}U/^{238}U$ ratios that are incompatible with the moderate and high ratios seen in ground and surface waters.

4 DISCUSSION

4.1 Surface and Groundwaters Influenced by Common Source

The fact that Treasure Valley ground and surface waters are connected is not, in itself, a novel discovery (Petrich & Urban, 2004). Yet there are some questions about the amount of association with respect to dissolved uranium dynamics between the two systems. The findings of this study provide evidence against the presence of a deep aquifer uranium source, while also challenging the existence of a purely surficial source (e.g., loess mantle, topsoil, and fertilizer). A somewhat more complicated scenario appears to exist where groundwater and surface waters are both affected by a similar shallow geologic (or near-surficial) source, and where shallow groundwater may be a significant source of uranium to downstream surface waters.

While plots of uranium concentration vs depth for the existing agency dataset do not particularly show the absence of high uranium at greater depths (Figure 3), there are questions surrounding both the temporal variability of the this dataset and the true accuracy of the depth estimates that give sufficient cause to question the validity of the relationship shown. By contrast, a trend of higher uranium concentrations at shallower depths exists for the set of wells sampled for this study. Although small, this study's dataset does, however, provide the advantage of lower temporal and spatial variability when compared to the existing agency data. Another recent Treasure Valley study (Cosgrove & Taylor, 2007) reports a supporting qualitative trend of high uranium at

relatively shallow depths and low uranium in all deep aquifer samples. This potential correlation between uranium concentration and depth points towards a more surficial source location.

Isotopic data from the solid extractions experiments (Figure 14) show that solids representative of deeper aquifer sediments consistently yield low $^{234}U/^{238}U$ ratios that are incompatible with the contamination source, as did the suspected surficial uranium sources. These results provide strong evidence for excluding deep aquifer formations, surface loess, and fertilizers as uranium sources. In fact, the only solids found to be potentially isotopically compatible with the contamination source came from samples representing vadose zone and shallow aquifer locations, as will be discussed further (Section 4.3).

A consistent seasonal signal can be seen in both uranium concentrations and isotopic concentrations of several Treasure Valley surface waters. Higher Boise River uranium concentrations occur during the winter season than the summer irrigation season. The high winter season uranium signal is even seen in Indian and 10 Mile Creeks, which are the most heavily influenced by irrigation return flows (Table 2). This trend is important considering that shallow groundwater discharging to surface water channels is expected to comprise a greater proportion of total surface water flows during the winter season, suggesting that high uranium conditions of the winter sampling are largely due to fluxes from shallow groundwater. This interpretation is also supported by the coupled fact that each of the previously mentioned surface waters also displays an isotopic shift in downstream compositions. Each body's winter season sample evolves to relatively higher

$^{234}U/^{238}U$ and lower $^{87}Sr/^{86}Sr$ ratios than in summer sampling. This shift is more isotopically consistent with the observed mean groundwater composition (Figure 7).

The final key piece of evidence for the interconnectedness of Treasure Valley surface and groundwater systems with respect to uranium dynamics is the congruence of their respective isotopic compositions. The groundwater samples show diverse isotopic compositions in low uranium samples and samples from spatially distal edges of the study area (Figure 11) but converge toward a common region of isotopic space at higher uranium concentrations (Figure 12). Surface waters show somewhat different isotopic evolution dynamics, but still converge toward a similar isotopic space as they become more concentrated in uranium (Figure 8). The Boise River and Indian and 10 Mile Creeks all begin upstream with $^{234}U/^{238}U$ and $^{87}Sr/^{86}Sr$ values that lie outside of the cluster of groundwater compositions (Figure 11). But they each ultimately evolve downstream toward isotopic compositions similar to that of the approximate weighted mean groundwater composition. In fact, downstream Boise River and 10 Mile Creek samples share strikingly similar isotopic compositions with two of the highest uranium groundwater samples. The combined elemental and isotopic results of ground and surface waters and solids extractions provide strong evidence that the source of uranium to Treasure Valley waters is best described as a shallow geologic source, but likely not as surficial as loess mantle deposits. The shallow nature of the source means that ground and surface water systems can be affected by isotopically similar uranium contributions. This phenomenon can be explained either by each system directly interacting with the source material or by shallow groundwater conveying the source uranium to surface waters, or by a combination of both processes. The source's isotopic signature is best

approximated as the isotopic region toward which the Boise River, Indian Creek, and 10 Mile Creek all evolve, and within which highly contaminated and weighted mean groundwater compositions exist.

4.2 Interpretation of Solids Extraction Results

The spatially distributed, but sporadic, nature of elevated uranium in the groundwater of the Treasure Valley (Figure 2) suggest that the source of (or the conditions for) uranium release may not exist ubiquitously, but rather in specific locations or stratigraphic depths. A wide variety of solids representing aquifer materials were tested for their ability to release uranium, and specifically for their ability to produce isotopic signatures matching that of the proposed contamination source. Each solid sample was exposed to three different selective extractant and a total dissolution in order to gain insight into specific mineral phases or geochemical processes important to uranium release.

Although bulk Treasure Valley aquifer sediments are not particularly uranium-rich, it can be seen that some localized sediments may have the ability to become secondarily enriched in uranium through physical or chemical processes, such as sorption, complexation, or evaporative enrichment. Several solids samples were considerably more pronounced than the rest in their ability to release uranium. Given that uranium is commonly known to have a strong affinity for complexing with carbonates (Baeza et al., 2008; Elless & Lee, 1998) and that clays and iron oxides tend to be highly capable of uranium sorption (Ames et al., 1983; Taboada et al., 2006; Porecelli & Swarzenski, 2003), it is not surprising that the list of highest uranium-releasing solids was largely dominated by carbonate-rich, iron oxide-rich, and fine grained samples

(Table 5). However, most of highest uranium releasing solids, and the clear majority of all analyzed solids, yielded leachates with $^{234}U/^{238}U$ ratios clearly too low to match the contamination source. The high uranium solids still support the important roles that Treasure Valley carbonates and iron oxides can play in uranium mobilization, but also highlight the fact that few solids demonstrate the ability to release significant uranium and even fewer can potentially match the isotopic signature of the uranium source.

The widespread low $^{234}U/^{238}U$ ratios yielded by most of the analyzed solids is the primary factor limiting them from consideration as potential Treasure Valley uranium sources (Figure 14). Most geologic materials are old enough that their age-dependent $^{234}U/^{238}U$ ratios have reached (or are very close to) secular equilibrium. Therefore, the ability of a solid at secular equilibrium to yield a leachate with a $^{234}U/^{238}U$ value significantly above the equilibrium level can either indicate that the solid is very young, or more commonly that the solid is sufficiently old enough to have undergone many half-lives worth of ^{238}U decay (and accumulated the related radiation damage) without yet having experienced so much environmental weathering that the solid is profoundly leached of all resulting ^{234}U. In the case of all of the deep aquifer solids (Chalk Hills, Glenns Ferry, and Pierce Gulch formations), the true age of formation of their sedimentary clasts is difficult to determine. Yet each formation is identified as being deposited during the Tertiary period, establishing that their parent materials must be ≥ about 2.5 million years old, most likely being much older. Therefore, each of the deep aquifer samples would be expected to plot near the $^{234}U/^{238}U$ secular equilibrium level, based on whole rock chemistry. Given that natural aquifer leaching is not nearly aggressive enough to completely dissolve sediments, solid analysis by complete

dissolution would not be an appropriate analog for in situ conditions. The selective extraction experiments were designed to simulate three different leaching scenarios that are based on geochemical conditions that that aquifer solids could conceivably encounter. Depending on the aggressiveness of the extraction treatment and how well it serves to target specific minerals within the various solids, the sets of three isotopic data points for each solid sample provide a range (generally being most variable in the $^{234}U/^{238}U$ component) that approximates the possible isotopic compositions of the weathering products released as a result of leaching each solid.

The more surficial samples may have been deposited more recently than the deep aquifer samples, but their parent materials are not necessarily younger than the sediments they overlay. This principle is exemplified by the fact that loess samples, the most surficial solids collected, yield isotopic ratios that are on par with the low $^{234}U/^{238}U$ values of the deep aquifer solids. However, two different shallow sediment formations were the sites from which the only two high $^{234}U/^{238}U$ solid samples were found. Sample 1#4, a silty clay sample with visible iron oxide staining from the Gowen Terrace, produced leachates with the highest $^{234}U/^{238}U$ ratios and overall $^{234}U/^{238}U$ and $^{87}Sr/^{86}Sr$ ratios most congruent with the uranium contamination source. Sample 7#1, a silty sample extracted from a core into the modern floodplain, yielded a high $^{234}U/^{238}U$ and high uranium leachate from its carbonate extraction. The other two extractants produced much lower $^{234}U/^{238}U$ ratios for sample 7#1.

No stratigraphic evidence was observed that suggests a stark change in parent material between samples 1#4 and 1#5. The two silty clay layers were immediately adjacent to each other with 1#4 sitting conformably atop 1#5. As the presence of iron

oxide staining in sample 1#4 was the only discernable difference between the two samples, it is logical to suspect that the considerably higher $^{234}U/^{238}U$ ratios from sample 1#4 may be related to sample 1#4 containing a distinct reservoir of uranium associated with its iron oxide surfaces. A similar scenario exists with samples 7#1 and 7#2. These two samples were not found stratigraphically adjacent to each other, but were in a close proximity and were composed of similarly silty textures. However, the leachates from the two samples yielded quite different isotopic compositions. Sample 7#2's leachates all plot in a cluster that is consistent with the range of low $^{234}U/^{238}U$ values found from the majority of solids. Sample 7#1 stands out as its carbonate extraction produced a particularly high $^{234}U/^{238}U$ ratio, while its other two extractions produced very low $^{234}U/^{238}U$ values. The wide disparity between sample 7#1's carbonate leachable isotopic composition and its DI water and iron oxide leachable isotopic composition can be interpreted as showing that 7#1's sediments are overall quite weathered and likely to produce whole rock isotopic compositions with low $^{234}U/^{238}U$ ratios, but that the sample still possesses a significant reservoir of higher $^{234}U/^{238}U$ uranium that can be liberated specifically by the carbonate extractant. Similar to sample 1#4, sample 7#1 does not appear to contain unique sedimentary materials that are responsible for releasing high $^{234}U/^{238}U$ ratios. Instead, each sample may be seen as containing traces of high $^{234}U/^{238}U$ uranium that was originally released by a yet unidentified source, but which is now coated to surfaces, sorption sites, and ion exchange sites associated with shallow non-source sediments. In this scenario, the original uranium source would logically be constrained to shallow sediments situated up-gradient from the locations where high $^{234}U/^{238}U$ traces were discovered, meaning that uranium was originally released from

profoundly shallow materials before being partially detained by the fine grained sediments exemplified by samples 1#4 and 7#1.

4.3 The Role of Carbonates in Uranium Mobility

The role of carbonates as being the preferred complexing partner for maintaining uranium's solubility in aqueous systems is widely known (Baeza et al., 2008; Elless & Lee, 1998). In Treasure Valley ground and surface waters, uranium concentrations are positively correlated with alkalinity, with the groundwater uranium vs alkalinity relationship representing a particularly strong trend (Figure 5; Figure 9). MINTEQ geochemical modeling confirms that several uranyl-carbonate complexes comprise, on average, about 99% of dissolved uranium in Treasure Valley waters, supporting the vital role of alkalinity in promoting uranium release and mobility, both through carbonate mineral dissolution and desorption by increasing effective solubility.

Solid extraction results show that the importance of the association between uranium and carbonates extends to the solid phase as well. Most of the highest leachable uranium content values, and the highest average uranium content value were produced by the carbonate extraction scenario (Table 5; Figure 13). These trends would seem to indicate that carbonate-rich sediments are acting as the source of uranium contamination in the Treasure Valley. But upon closer inspection of the data, several discrepancies appear to challenge this interpretation. Among all of the solids collected, three (samples 1#2, 2#1, and 4#2) were observed to contain significant carbonate mineral contents. The presence of particularly high $CaCO_3$ concentrations in the three samples is further confirmed by the clear spikes in calcium resulting from the carbonate extractions of these samples (Figure 13). Although each of the carbonate-rich samples demonstrates the

ability to release relatively high levels of uranium, none of them yield isotopic compositions that are compatible with the uranium contamination source (Figure 14). These three samples show that surficial carbonate horizons and calcareous formations have the ability to accumulate high concentrations of uranium, but that it can't be presumed that these carbonate-rich materials act as the primary uranium sources in the Treasure Valley. However, surficial carbonates are likely still important as donators of dissolved carbonate, thus promoting enhanced uranium solubility in the shallow aquifer. Looking past the three carbonate-rich solid samples, several other of the highest uranium values (1#1, 3#1, 5#2, and 7#1) were produced through carbonate extractions, even though none of those solids are particularly carbonate-rich. Also, it can be seen that the carbonate extraction was able to release uranium about as well as the iron oxide extraction did for samples with obvious iron oxide staining (1#4, 3#1, and 4#3). This release of uranium is also accomplished while only releasing a fraction of the iron seen in the iron oxide extractions of the same sample. If the extraction designed to target carbonate minerals also shows better efficiency than the more aggressive iron oxide extraction when it comes to releasing uranium from most solids without a substantial carbonate component, then there are two reasonable hypotheses that may explain the observed behavior: (1) Minor amounts of carbonate cement, ubiquitous to nearly all solids, represents the primary reservoir of uranium, or (2) the mere presence of small concentrations of carbonate in the leachate solutions is enough to efficiently release uranium bound to the solids via sorption and/or ion exchange sites, increasing the effective solubility of uranium. This second scenario can be referred to a carbonate-assisted leaching. The case for carbonate-assisted leaching is supported by the fact that

the carbonate extraction also demonstrates the ability to most effectively release potassium from the clear majority of the solid samples. This trend, especially in the cases of potassium release from fine grained sediments, can be a signal of cation exchange from clay components. Additionally, when considering the two solids that yield isotopic compositions potentially compatible with the uranium contamination source (samples 1#4 and 7#1), potassium is among the elements that show an increase in concentration positively correlated with $^{234}U/^{238}U$ ratios throughout the three extraction scenarios (Figure 16). At least in the case of samples 1#4 and 7#1, the uranium release may well be attributed to clays that are also releasing exchangeable potassium.

While several pieces of evidence support the theory of carbonate-assisted leaching, it is unclear whether pH conditions present in the carbonate extraction scenarios were high enough to allow for the specific presence of dissolved CO_3^{2-} or HCO_3^-. At the neutral to slightly alkaline pH conditions of environmental samples, carbonate-assisted leaching would be quite plausible, with pedogenic carbonates and other carbonate rich surficial materials likely acting as sources of dissolved carbonate to the shallow aquifer. However, in the strongly acidic pH range, carbonate speciation would be dominated by H_2CO_3. Unfortunately, resulting pH values for leachates were not measured, and it is unknown whether the acetic acid extractant solutions (starting at pH 4.5) underwent pH change prior to mixing with solids. A future investigation could test for carbonate-assisted leaching by reacting solids with a neutral to alkaline HCO_3^- extractant.

Independent of the fact that the carbonate extraction produces the highest leachable uranium contents, the same extraction also yields the highest average $^{234}U/^{238}U$ ratios (Figure 15). The ability to produce leachates with higher $^{234}U/^{238}U$ values is

especially important since low $^{234}U/^{238}U$ isotopic composition is the primary limiting factor preventing all but two solid samples from potentially matching the isotopic signature of the uranium contamination source. Exactly how the solid samples react with each extractant to produce a given $^{234}U/^{238}U$ ratio is something that is different for every sample, and depends on a complex combination of factors, including (but not limited to) the solid sample's lithology, texture, and age. But there are some relationships between extraction scenarios and relative $^{234}U/^{238}U$ ratios that hold true for the majority of the solid samples. The DI water extraction will generally only be able to access the outer rind of each solid grain without the aggressiveness to undertake significant geochemical exchange with solid surfaces or dissolve the resistant solid matrix. If the solids that the DI water interacts with have not been sufficiently weathered, the DI water can selectively leach only the most easily mobilized uranium reservoir. The reservoir would be enriched in ^{234}U relative to the whole rock $^{234}U/^{238}U$ composition. However, most of the sediments sampled are highly weathered. In such cases, the solid rinds have previously had most of their ^{234}U leached away, resulting in DI water leachates that are near the whole rock $^{234}U/^{238}U$ ratio or even lower. The three solid leachate samples that plot below the secular equilibrium level are examples of DI water interacting with old, highly weathered solids (Figure 14). The iron oxide extraction scenario produces $^{234}U/^{238}U$ ratios that are, on average, similar to but slightly higher than those produced by DI water leaches. The iron oxides extractant's low pH and reductive capacity allow it to aggressively attack more resistant portions of the solid matrix. As the iron oxide extractant is the most aggressive in solid dissolution, it produces $^{234}U/^{238}U$ ratios nearest to the whole rock values without ever yielding $^{234}U/^{238}U$ ratios below the secular equilibrium level. The carbonate

extraction scenario is able to typically produce the highest $^{234}U/^{238}U$ ratios from a given solid because, unlike the iron oxide extractant, it is able to mildly penetrate solid rinds (especially by dissolving carbonate mineral phases) and access previously unweathered ^{234}U sites without being so destructive as to achieve wholesale dissolution of uranium-bearing minerals with near secular equilibrium $^{234}U/^{238}U$ ratios. The carbonate extractant is also more reactive than DI water when it comes to accessing the uranium associated with solid surfaces, and can aid desorption and ion exchange of uranium from this reservoir by supplying dissolved carbonate as a preferential complexing partner for uranium. While the DI water extraction was originally intended to target the water soluble fraction of solid samples, highly purified water, as opposed to a solution containing dilute salt or bicarbonate concentrations, may have been too inert to leach uranium at an aggressiveness level that is on par with actual environmental conditions.

4.4 The Isotopic Incompatibility of Fertilizers

While two of the three fertilizer samples tested did exhibit sufficiently high uranium contents to be potentially implicated as significant uranium sources (Table 4), their isotopic signatures are simply not compatible with the $^{234}U/^{238}U$ ratios observed in Treasure Valley waters (Figure 14). The moderate to high $^{234}U/^{238}U$ compositions of groundwater and downstream surface water samples are indicative of water-rock interaction scenarios where preferential leaching of ^{234}U leads to $^{234}U/^{238}U$ ratios well above the secular equilibrium. By contrast, fertilizer dissolutions released uranium at the equilibrium level; very much on par with the whole-rock compositions of the phosphate ore samples. In the case of all other geologic solids analyzed, isotopic compositions of whole-rock dissolutions would not be valid representations of environmental weathering

of the solids as environmental waters do not completely dissolve the rocks with which they interact. However, in the case of fertilizer products, the solids are specifically designed to be completely soluble, thus validating the use of fertilizer dissolution data.

4.5 Possible Areas for Further Study

If the findings of this study were to lead to additional research, further discovery could foreseeably come from the results of additional sampling and analysis efforts. Additional serial sampling of the Boise River (and potentially Indian and 10 Mile Creeks as well) with an increased number of sample sites would allow for a more precise estimation of what/where the source of uranium to the river is. Additional sampling of decidedly distributed high uranium groundwater wells would allow for more robust analysis of geochemical trends. Of particular interest would be the investigation of apparent bifurcations seen in the groundwater elemental data (Figure 9; Figure 10), and their potential to be correlated to the diversity of uranium isotopic end-members expressed in groundwater samples (Figure 12). Finally, future solid sampling and analysis would be best served to focus on collecting additional shallow, fine grained sediments from modern alluvial deposits and relatively young terrace formations. The highest $^{234}U/^{238}U$ ratios discovered were those associated with the waters of the upstream Owyhee River and with a municipal well in Kuna (Figure 11). To find the lithologic origin of the high $^{234}U/^{238}U$ ratios, solids derived from the rhyolitic Owyhee Range and shallow sediments from the Kuna area would each be high priority samples to analyze. As mentioned previously, an amendment to improve the selective extraction methods would be to leach solids with a dilute bicarbonate solution in order to better assess the carbonate-assisted leachable fraction of a given solid.

5 CONCLUSIONS

The analysis of solids representing Treasure Valley aquifer materials uncovered several shallow alluvial formations with lithologies capable of yielding isotopic compositions compatible with the Treasure Valley uranium contamination source. Significant evidence was found to both discount several potential sources and to significantly constrain the possible locations and lithologies of uranium source materials. Surface and groundwater sampling results helped create a preliminary depiction of the isotopic character the Treasure Valley's waters while also providing information about the nature of interconnections between dissolved uranium concentrations in the surface and aquifer systems. Finally, geochemical relationships and trends involving groundwater uranium were discovered, which may shed light on the release and behavior of uranium in the Treasure Valley and other such environments.

5.1 Near Surface Uranium Source

Several key pieces of evidence suggest that the primary input of uranium to the Treasure Valley system is represented by a shallow geologic source. Uranium concentrations in the Lower Boise River were found to increase approximately 18-fold from between the upstream and downstream sampling locations used in this study. Along this reach, inputs to the river include: streams draining the foothills north of the river, streams draining the largely agricultural lands south of the river, and shallow groundwater recharging to the river channel. Among streams sampled, tributaries from

the northern foothills demonstrated low uranium concentrations and low $^{234}U/^{238}U$ ratios, both qualities being inconsistent with the contaminated ground and surface waters. By contrast, the tributaries from south of the river contained the highest observed uranium concentrations while also yielding $^{234}U/^{238}U$ and $^{87}Sr/^{86}Sr$ ratios compatible with the contaminated waters. Mass balance between the Boise River uranium loads and those of the southern tributaries suggests that it is highly unlikely that the tributaries alone supply enough uranium to produce the high concentrations observed in the downstream Boise River. While the explicit measurement and characterization of groundwater recharging the river channel was outside of the scope of this study, it is almost certain that shallow groundwater inputs to the river represent a significant proportion of the downstream uranium increases. The case for shallow groundwater flows supplying uranium to the surface is further strengthened by the fact that seasonal sampling revealed a consistent trend of significantly higher uranium concentrations occurring during winter sampling (when a greater proportion of all surface waters are coming from shallow groundwater return) compared to summer sampling.

Additional evidence of a shallow uranium source can be seen in the isotopic compositions of aquifer solid leachates. Four sampling locations were dedicated to the collection of solids representative of the ancient lake sediments that comprise the deeper Treasure Valley Aquifer units. None of the sample lithologies from these locations could produce $^{234}U/^{238}U$ ratios matching the contaminated waters. The only solid samples with leachates matching the isotopic character of the contaminated waters were found within river terrace and floodplain sediments that house the shallow aquifer and are exposed to uranium originating near the surface.

5.2 Isotopic Similarity in Contaminated Ground and Surface Waters

The common area of $^{234}U/^{238}U$ and $^{87}Sr/^{86}Sr$ space towards which the Boise River and its southern tributaries each evolve represents the approximate isotopic signature of the material(s) acting as the source of uranium release to the surface. Additionally, the nearby Owyhee River (which at its upstream reaches exhibits a dramatically different isotopic composition than that of the Boise River and which can be considered hydrologically unconnected from the Boise River due to the fact that it lies to the west of the Snake River) also evolves towards an isotopic composition similar to that of the downstream Boise River's uranium source. The fact that these two separate rivers originate from very different headwater geologies but still evolve towards similar isotopic compositions as they increase their interaction with Treasure Valley sediments suggests that the uranium source is distributed throughout the valley, if not the Western Snake River Plain. Not only do multiple surface waters converge towards the contamination source signature, heavily contaminated groundwater samples and overall mean groundwater isotopic compositions also plot near this common isotopic composition nexus. Among the three highly contaminated groundwater samples (>50 $\mu g\ L^{-1}$), two were found to be almost isotopically identical to downstream Boise River waters. The uranium mixing relationship for groundwater samples is not as simple as it is for surface waters due to the fact that surface waters exhibit two component mixing curves while groundwater data show mixing from more diverse end-members. However, it can still be seen that surface waters appear to all be evolving towards the range of isotopic compositions of higher uranium groundwater and mean groundwater. This common area of isotopic convergence defines the signature of the proposed contamination source.

5.3 Phosphate Fertilizer Cannot Be the Uranium Source

Although the total dissolution of three phosphate fertilizer products and two phosphate ore rock samples confirmed that phosphate materials do indeed contain high quantities of uranium, there is no evidence to support the hypothesis that the application of phosphate fertilizers is causing uranium contamination in Treasure Valley waters. The $^{234}U/^{238}U$ ratios of all phosphate fertilizer and ore samples indicate secular equilibrium conditions: $^{234}U/^{238}U$ ratios that are far too low to be implicated as the contamination source.

5.4 Carbonate Dissolution and Carbonate-Assisted Leaching Yield the Highest Uranium Concentrations and Present the Best Isotopic Fit to the Contamination Source

The three different selective extraction scenarios applied to each solid sample produced different quantities of leachable uranium and different $^{234}U/^{238}U$ ratios. The water soluble extraction consistently released very little uranium. On the other extreme, the iron oxide extraction was designed to be a more aggressive leaching scenario, and therefore released significant quantities of uranium from the solids. The iron oxide extraction accomplished the reductive dissolution of several metal oxides as well as the destruction of more resistant portions of solid matrices. Neither of these qualities is believed to be applicable to environmental conditions commonly observed in Treasure Valley surface and shallow aquifer conditions. The carbonate extraction may represent the best surrogate for in situ uranium leaching conditions. Although acetic acid isn’t widely found in nature, the mild acidity of meteoric water is similarly able to release dissolved carbonate from pedogenic carbonates and other surficial carbonate sources. The

highest values for leachable uranium and highest average $^{234}U/^{238}U$ ratios came from the carbonate extraction. In addition to releasing uranium from solid samples that were known to be high in carbonate content, the carbonate extraction also released significant uranium from solids that were not carbonate-rich and even from solids that were markedly iron oxide-rich. In these latter cases, the uranium being released is likely desorbed or exchanged from iron oxide and clay surfaces once a more preferable complexing agent is made available through the dissolution of even small amounts of carbonates within the sediments. The strong correlation between uranium and alkalinity in both ground and surface water samples only supports the importance of carbonate-assisted leaching as being the primary mechanism of uranium mobilization in the Treasure Valley. The carbonate-assisted leaching scenario describes a situation where uranium of high $^{234}U/^{238}U$ character is detained on the surfaces of shallow, reactive sediments, only to be later released when exposed to fluxes of higher carbonate waters emanating from the surface. This scenario is likely exemplified by samples 1#4 and 7#1. As the two samples do not appear to contain unique sedimentary materials that explain their high $^{234}U/^{238}U$ ratios, the solids may be best described as containing traces of high $^{234}U/^{238}U$ uranium that was originally released by a yet unidentified source, but which is now coated to surfaces, sorption sites, and ion exchange sites associated with shallow non-source sediments.

REFERENCES

Ames, L.L., J. E. McGarrah, B. A. Walker. 1983. Sorption of Trace Constituents from Aqueous Solutions onto Secondary Minerals: Uranium. *Clays and Clay Minerals* 31 (5): 321-334.

Andersen, M.B., Y. Erel, B. Bourdon. 2009. Experimental Evidence for ^{234}U–^{238}U Fractionation During Granite Weathering With Implications for $^{234}U/^{238}U$ in Natural Waters. *Geochimica et Cosmochimica Acta* 73: 4124–4141.

Baeza, A., A. Salasa, F. Legarda. 2008. Determining Factors in the Elimination of Uranium and Radium from Groundwaters During a Standard Potabilization Process. *Science of the Total* Environment 406: 24-34.

Blanco, P., F. Vera Tome, J.C. Lozano. 2005. Fractionation of Naturalized Radionuclides in Soils from a Uranium Mineralized Areas in the South-West of Spain. *Journal of Environmental Radioactivity* 79: 315-330.

Buck, E.C., N.R. Brown, N.L. Dietz. 1996. Contaminant Uranium Phases and Leaching at the Fernald Site in Ohio. *Environmental Science & Technology* 30: 81-88.

Busbee, M.W., B.D. Kocar, S.G. Benner. 2009. Irrigation Produces Elevated Arsenic in the Underlying Groundwater of a Semi-Arid Basin in Southwestern Idaho. Applied Geochemistry 24: 843-859.

Chabaux, F., J. Riotte, A. Schmitt, J. Carignan, P. Herckes, M. Pierret, H. Wortham. 2005. Variations of U and Sr Isotope Ratios in Alsace and Luxembourg Rain Waters: Origin and Hydrogeochemical implications. *Comptes Rendus Geoscience* 337: 1447–1456.

Clark, D.L., D.E. Hobart, M.P. Neda. 1995. Actinide Carbonate Complexes and Their Importance in Actinide Environmental Chemistry. *Chemical Reviews* 95: 25-48.

Clow, D.W., M.A. Mast, T.D. Bullen, J.T. Turk. 1997. Strontium 87/strontium 86 as a Tracer of Mineral Weathering Reactions and Calcium Sources in an Alpine/Subalpine Watershed, Loch Vale, Colorado.

Cosgrove, D.M., Taylor, J. 2007. Preliminary Assessment of Hydrogeology and Water Quality in Ground Water in Canyon County ID. *Idaho Water Resources Research Institute Technical Report* 07-001.

Dhoum, R.T., G.J. Evans. 1998. Evaluation of Uranium and Arsenic Retention by Soil from a Low Level Radioactive Waste Management Site Using Sequential Extraction. *Applied Geochemistry* 13(4): 415-420.

Elless, M.P., S.Y. Lee. 1998. Uranium Solubility of Carbonate-Rich Uranium-Contaminated Soils. *Water, Air, and Soil Pollution* 107: 147-162.

Faure, G., T.M. Mensing. 2005. *Isotopes: Principles and Applications*. John Wiley & Sons, Inc., Hoboken, New Jersey.

Gascoyne, M. 1989. High Levels of Uranium and Radium in Groundwaters at Canada's Underground Research Laboratory, Lac du Bonnet, Manitoba, Canada. *Applied Geochemistry* 4(6): 577-591.

Grzymko, T.J., F. Marcantonio, B.A. McKee, C.M. Stewart. 2007. Temporal Variability of Uranium Concentrations and $^{234}U/^{238}U$ Activity Ratios in the Mississippi River and Its Tributaries. *Chemical Geology* 243: 344–356.

Hutchings, J., C.R. Petrich. 2002. Ground Water Recharge and Flow in the Regional Treasure Valley Aquifer System Geochemistry and Isotope Study: University of Idaho, Idaho Water Resources Research Institute Technical Report IWRRI-2002-08, Boise, Idaho.

Idaho Department of Environmental Quality (IDEQ). 2010. Agency website: http://www.deq.idaho.gov/.

Idaho Department of Water Resources (IDWR). 2010. Agency website: http://www.idwr.idaho.gov/.

Jarvis, K.E., A.L. Gray, R.S. Houk. 1992. Handbook of Inductively Coupled Plasma, Blackie, London. pp. 196-200.

Jeon, S., T. Nakano. 2001. Geochemical Comparison of Stream Water, Rain Water, and Watershed Geology in Central Korea. *Water, Air, and Soil Pollution* 130: 739–744.

Johnson, T.M., D.J. DePaolo. 1994. Interpretation of Isotopic Data in Groundwater-Rock Sytems: Model Development and Application to Sr Isotope Data from Yucca Mountain. *Water Resources Research* 30 (5): 1571-1587.

Johnson, T.M., R.C. Roback, T.L. McLing, T.D. Bullen, D.J. DePaolo, C. Doughty, R.J. Hunt, R.W. Smith, L.D. Cecil and M.T. Murrell. 2000. Groundwater "Fast Paths" in the Snake River Plain Aquifer: Radiogenic Isotope Rations as Natural Groundwater Tracers. *Geology* 28 (10): 871-874.

La Force, M.J., S. Fendorf. 2000. Solid-Phase Iron Characterization During Common Selective Sequential Extractions. *Soil Science Society of America* 64: 1608-1615.

Langmuir, D. 1997. *Aqueous Environmental Geochemistry*. Upper Saddle River: Prentice-Hall, Inc. 1997.

Lide, D.R., H.P.R. Frederikse. 1995. *Handbook of Chemistry and Physics*. CRC Press, Boca Raton, Florida.

Luo, S., T. Ku, R. Roback, M. Murrell, T.L. McLing. 2000. In-situ Radionuclide Transport and Preferential Groundwater Flows at INEEL (Idaho): Decay-series Disequilibrium Studies. *Geochimica et Cosmochimica Acta* 64 (5): 867–881.

Maher, K., D.J. DePaolo, J.C.F. Lin. 2004. Rates of Silicate Dissolution in Deep-Sea Sediment: In Situ Measurement Using U-234/U-238 of Pore Fluids. *Geochimica et Cosmochimica Acta* 68 (22): 4629–4648.

Maher, K, D.J. DePaolo, J.N. Christensen. 2006. U–Sr Isotopic Speedometer: Fluid Flow and Chemical Weathering Rates in Aquifers. *Geochimica et Cosmochimica Acta* 70: 4417–4435.

Martin, R., D.M. Sanchez, A.M. Gutierrez. 1998. Sequential Extraction of U, Th, Ce, La and Some Heavy Metals in Sediments from Ortigas River, Spain. *Talanta* 46:1115-1121.

McKinley, J.P., J.M. Zachara, J. Wan, D.E. McCready, S.M. Heald. 2007. Geochemical Controls on Contaminant Uranium in Vadose Hanford Formation Sediments at the 200 Area and 300 Area, Hanford Site, Washington. *Vadose Zone Journal* 6: 1004–1017.

Osmond, J. K., H.S. Rydell, M.I. Kaufman. 1968. Uranium Disequilibrium in Groundwater: An Isotope Dilution Approach in Hydrologic Investigations. *Science* 162 (3857): 997-999.

Othberg, K. L., Stanford, L. R. 1992. Geologic map of the Boise Valley and adjoining area, Western Snake River Plain, Idaho. *Idaho Geological Survey, Geologic Map Series, Scale 1:100,000.*

Pabalan, R.T., D.R. Turner. 1997. Uranium (6+) Sorption on Montmorillonite: Experimental and Surface Complexation Modeling Study. *Aquatic Geochemistry* 2(3): 203-226.

Petrich, C. R., S.M. Urban. 2004. *Characterization of ground water flow in the lower Boise River Basin*. Idaho Water Resources Research Institute.

Porecelli, D., P.W. Swarzenski. 2003. The Behavior of U- and Th-series Nuclides in Groundwater. *Reviews in Mineralogy and Geochemistry* 52: 317-361.

Prikryl, J.D., A. Jain, D.R. Turner, R.T. Pabalan. 2001. UraniumVI Sorption Behavior on Silicate Mineral Mixtures. *Journal of Contaminant Hydrology* 47: 241-253

Riotte, J., F. Chabaux. 1999. ($^{234}U/^{238}U$) Activity Ratios in Freshwaters as Tracers of Hydrological Processes: The Strengbach Watershed (Vosges, France). *Geochimica et Cosmochimica Acta* 63 (9): 1263–1275.

Roback, R. C., T. M. Johnson, T. L. McLing, M. T. Murrell, S. D. Luo, T. L. Ku. 2001. Uranium Isotopic Evidence for Groundwater Chemical Evolution and Flow Patterns in the Eastern Snake River Plain Aquifer, Idaho. *Geological Society of America Bulletin* 113(9): 1133-1141.

Schmitz, M.D, S.A. Bowring. 2001. U-Pb Zircon and Titanite Systematics of the Fish Canyon Tuff: An Assessment of High-Precision U-Pb Geochronology and Its Application to Young Volcanic Rocks: *Geochimica et Cosmochimica Acta* 65:2571-2587.

Schultz, M.K., W.C. Burnetta, K.G. Inn. 1998. Evaluation of a Sequential Extraction Method for Determining Actinide Fractionation in Soils and Sediments. *Journal of Environmental Radioactivity* 40 (2): 155-174.

Smith, D.K. 1984. Uranium Mineralogy. In Uranium Geochemistry, Mineralogy, Geology, Exploration and Resources. F. Ippolito, B. DeVero, G. Capaldi (Eds) Institution of Mining and Metallurgy, London, 43-71.

Squires, E. & Wood, S. H. 2001. *Stratigraphic Studies of the Boise (Idaho) Aquifer System Using Borehole Geophysical Logs with Emphasis on Facies Identification of sand Aquifer*s. Prepared for the Treasure Valley Hydrologic Study, Idaho Department of Water Resources.

Steiger, R.H., E. Jäger. 1977. Subcommission on Geochronology: Convention on the Use of Decay Constants in Geo- and Cosmochronology. *Earth and Planetary Science Letters* 36: 359-362.

Taboada, T., A.M. Cortizas, C. Garcia, E. Garcia-Rodeja. 2006. Uranium and Thorium in Weathering and Pedogenetic Profiles Developed on Granitic Rocks from NW Spain. *Science of the Total Environment* 356: 192– 206.

Taylor, M.D. 2007. Accumulation of Uranium in Soils from Impurities in Phosphate Fertilizers. *Landbauforschung Volkenrode* 57: 133-139.

Tessier, A., P.G.C. Campbell, M. Bisson. 1979. Sequential Extraction Procedure for the Speciation of Particulate Trace Metals. *Analytical Chemistry* 51(7)844-851.

Thoma, M.J., J.P. McNamara, M.M. Gribb, S.G. Benner. 2011. Seasonal Recharge Components in an Urban/Agricultural Mountain Front Aquifer System Using Noble Gas Thermometry. *Journal of Hydrology* (in press).

Thomas, R.P., A.M. Ure, C.M. Davidson, D. Littlejohn. 1994. Three-stage Sequential Extraction Procedure for Determination of Metals in River Sediments. *Analytica Chimica Acta* 286: 423-429.

Urban, S. M. 2004. *Water Budget for the Treasure Valley Aquifer System; Treasure Valley Hydrologic Project*. Idaho Department of Water Resources.

U.S. Environmental Protection Agency. 2009. *National Primary Drinking Water Regulations*; EPA 816-F-09-0004.

Wanty, R.B., D.K. Nordstrom. 1995. Natural Radionuclides. In *Regional Ground-Water Quality,* ed. W.M. Alley. Van Nostrand Reinhold. 1995.

Wood, S. H., Clemens, D. M. 2002. Geologic and tectonic history of the Western Snake River Plain, Idaho and Oregon. In B. Bonnichsen, C. M. White, M. McCurry, (Eds.) Tectonic and magmatic evolution of the Snake River Volcanic Province. *Idaho Geological Survey Bulletin 30*, 69-103.

Zielinski, R. A., S. Asher-Bolinder, A. L. Meier, C. A. Johnson, B. J. Szabo. 1997. Natural or Fertilizer-Derived Uranium in Irrigation Drainage: A Case Study in Southeastern Colorado, USA. *Applied Geochemistry* 12 (1): 9-21.

Zielinski, R. A., W. H. Orem, K. R. Simmons, P. J. Bohlen. 2006. Fertilizer-Derived Uranium and Sulfur in Rangeland Soil and Runoff: A Case Study in Central Florida. *Water Air and Soil Pollution* 176 (1-4): 163-183.

Zielinski, R. A., K. R. Simmons, W. H. Orem. 2000. Use of U-234 and U-238 Isotopes to Identify Fertilizer-Derived Uranium in the Florida Everglades. *Applied Geochemistry* 15(3): 369-383.

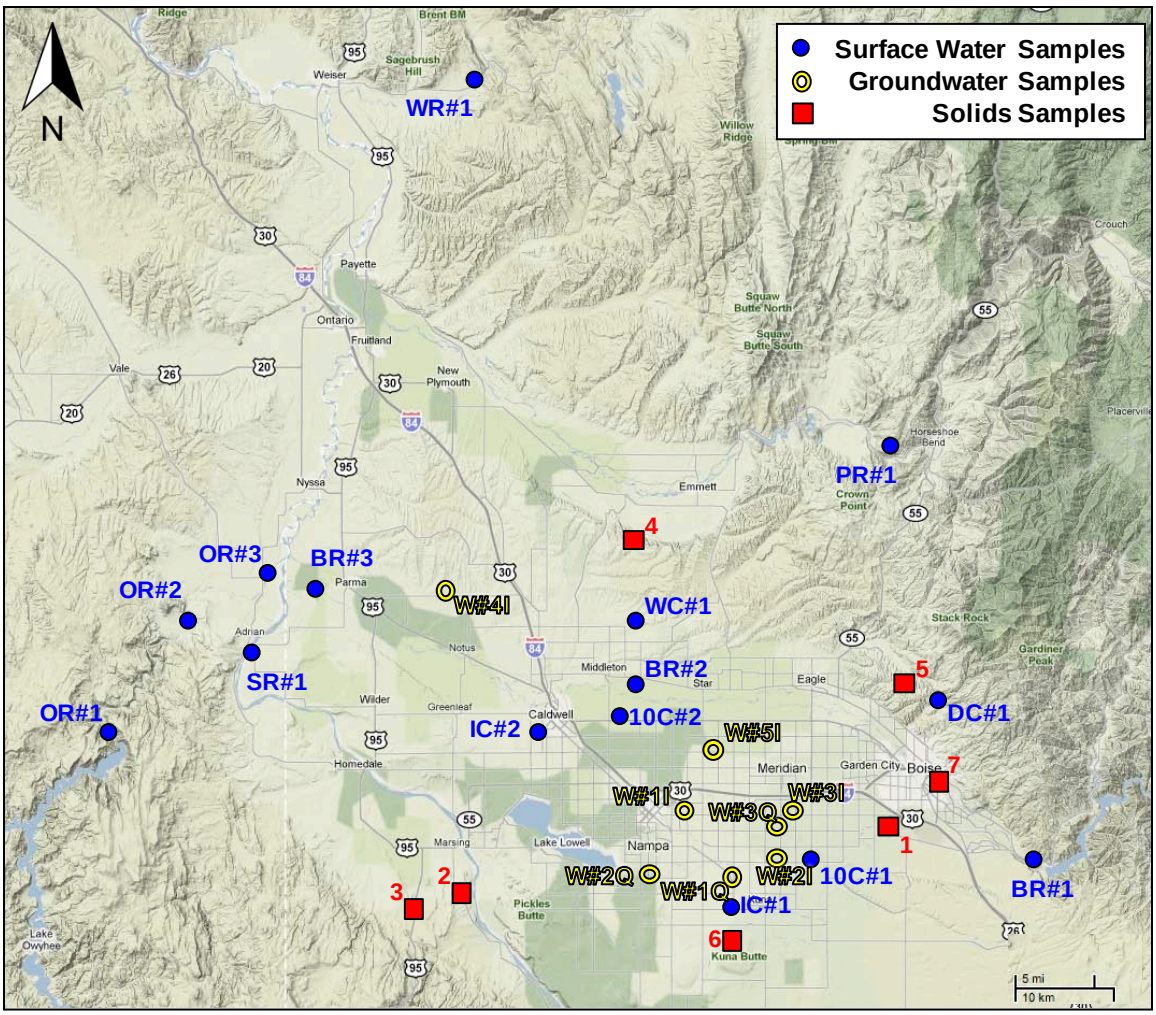

Figure 1: **Map showing the locations of: surface water samples (more details in Table 2), groundwater samples (Table 3), and solids samples (Table 4). Solids sample locations 1-6 represent sediment outcroppings while location 7 represents a well core of floodplain fill material.**

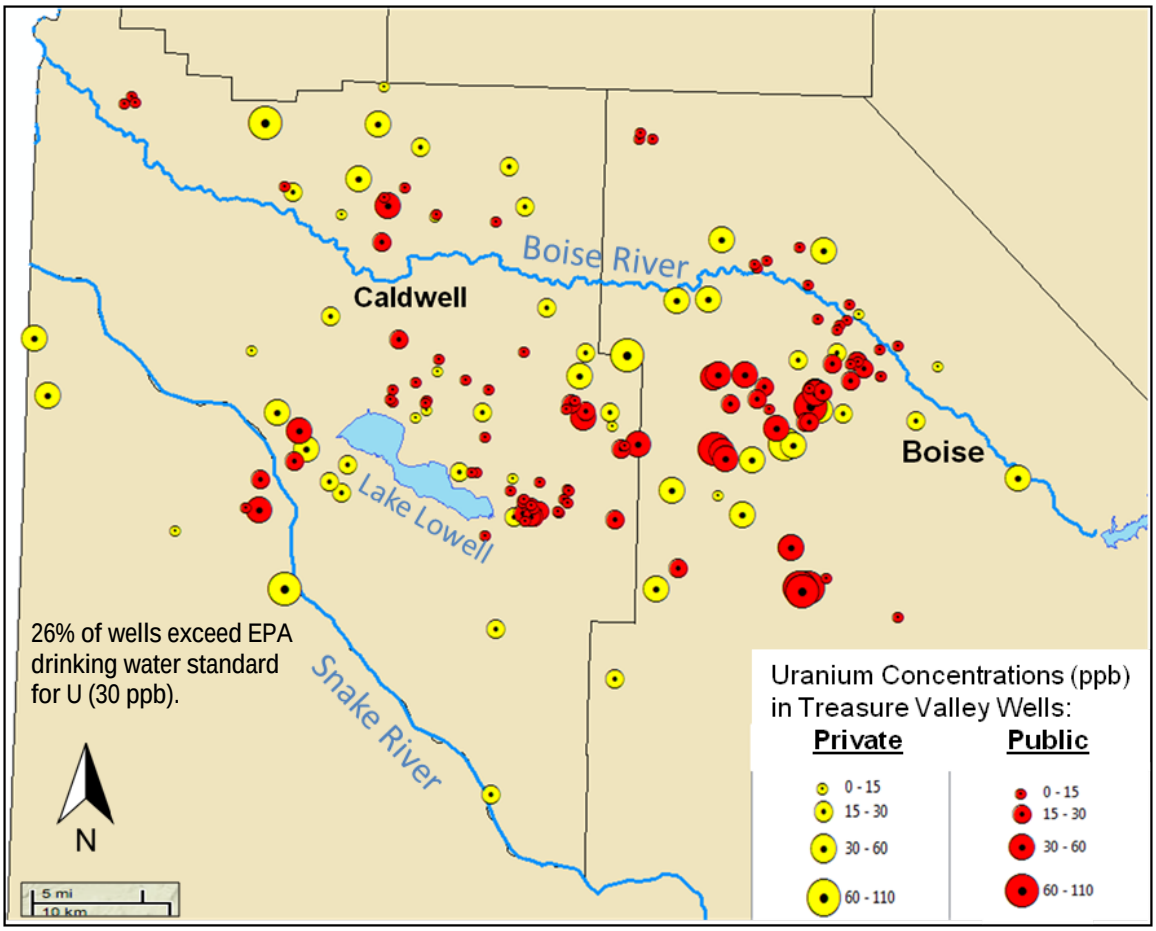

Figure 2: Groundwater uranium distribution map showing wells within the existing Public Water Systems (public) and Statewide Monitoring Network (private) datasets. Progressively larger circles indicate proportionally higher uranium concentrations in ppb notation (μg L^{-1}).

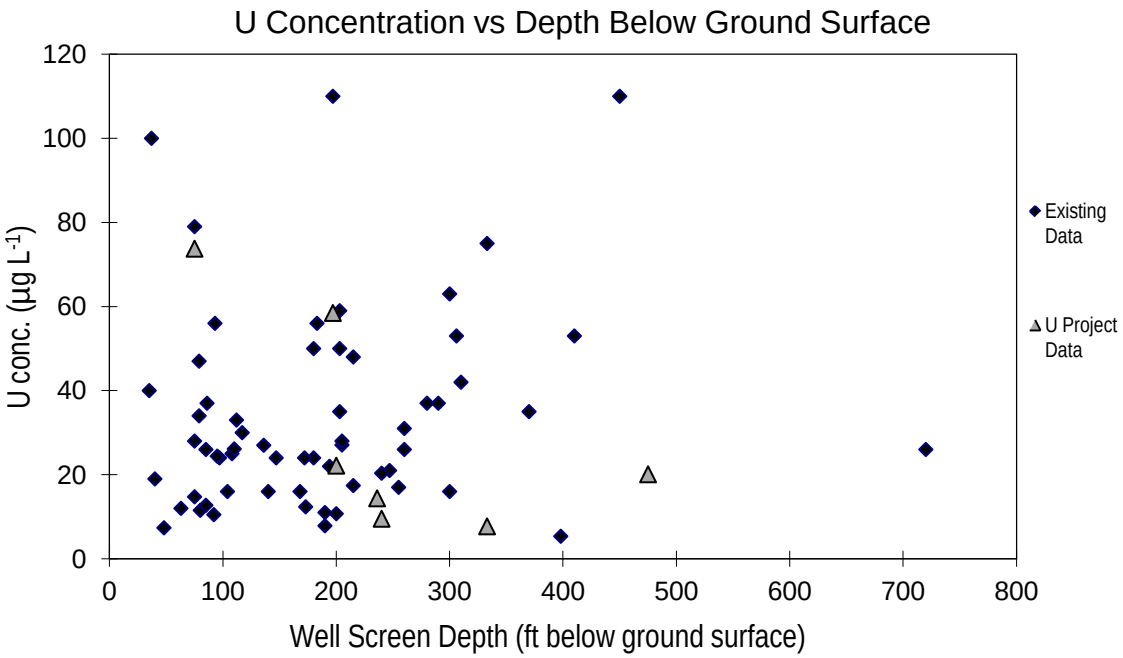

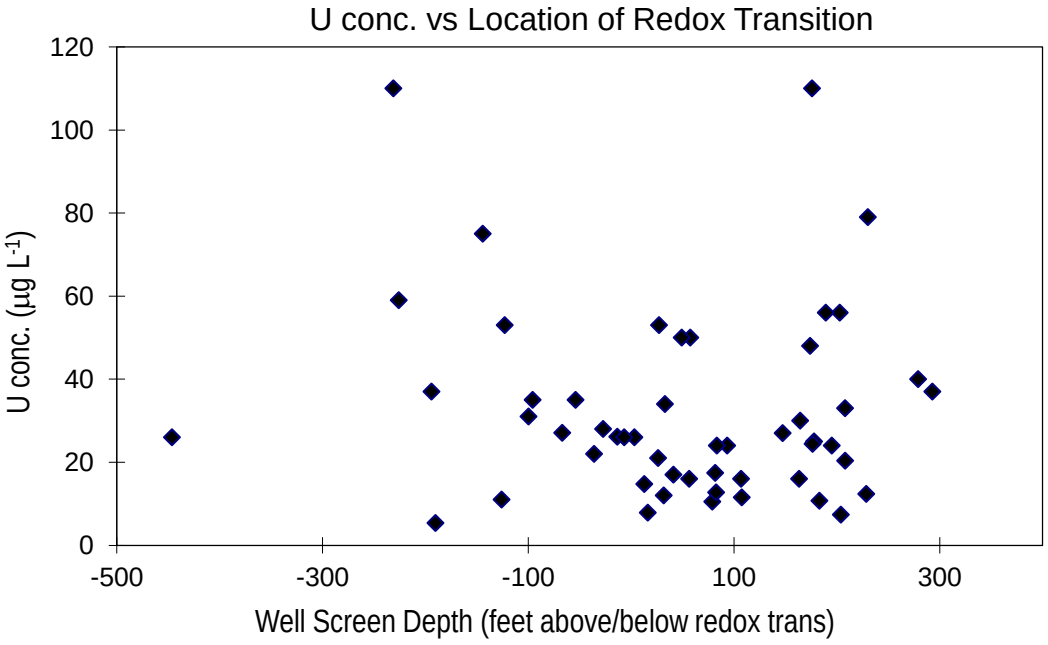

Figure 3: Groundwater uranium concentrations plotted against well depth (above) and against distance above/below the interpolated redox transition (below). The top plot includes the private well portion of the existing dataset and seven of the wells sampled for the current uranium project. Sample (W#3Q) was omitted as its well construction information could not be found. The bottom plot includes only the private well portion of the existing dataset. Location of redox transition determined using data from Busbee et al., 2009.

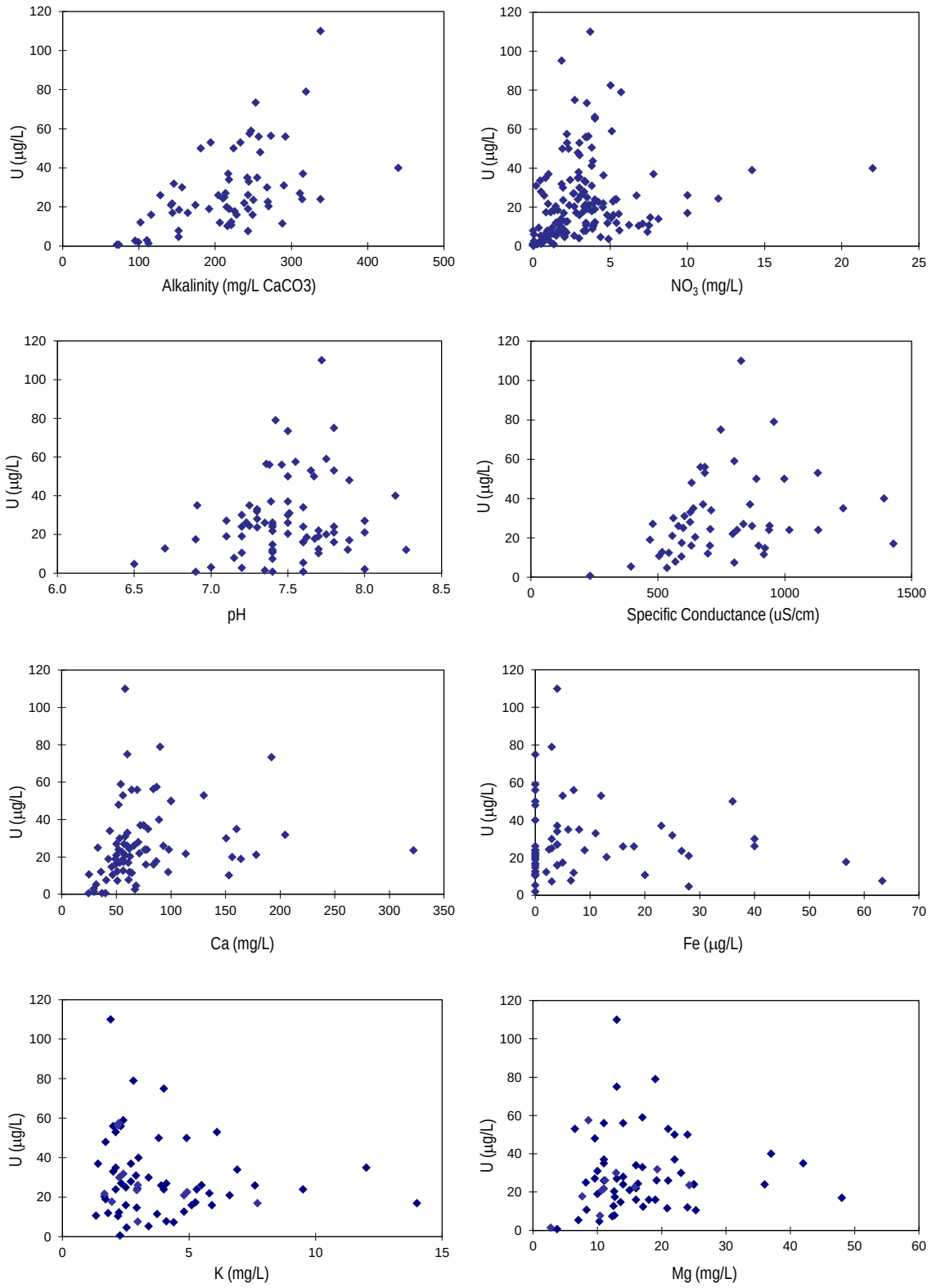

Figure 4: Groundwater uranium concentrations plotted against other dissolved species and parameters. All data are from existing agency dataset.

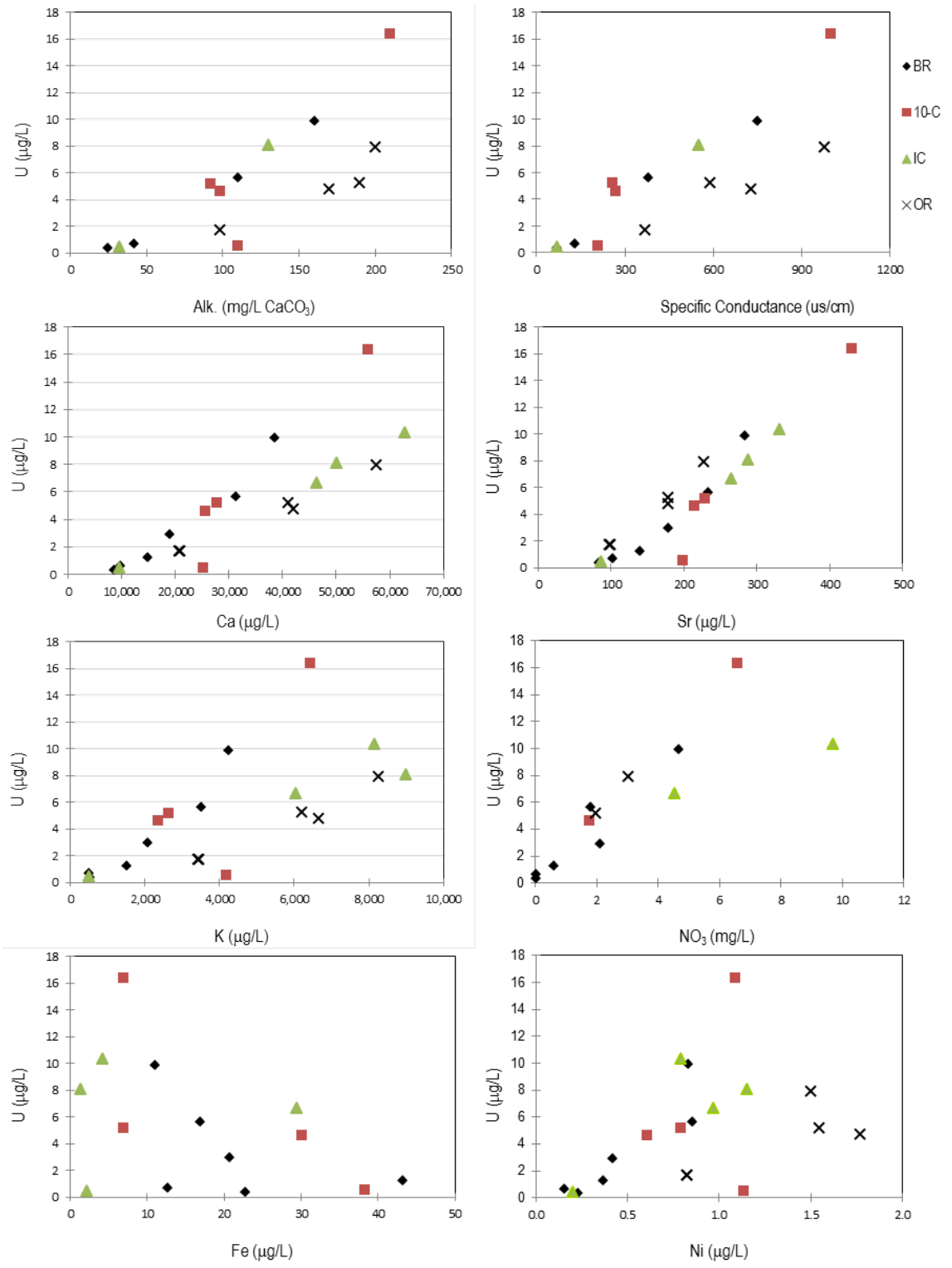

Figure 5: Surface water uranium concentrations plotted against other dissolved species and parameters. Data is plotted for synoptic sampling of: Boise River (BR), 10-Mile Ck. (10-C), Indian Ck. (IC), and Owyhee River (OR). Owyhee River samples are omitted from one plot to allow for focusing on the scale of the Boise River and its tributaries.

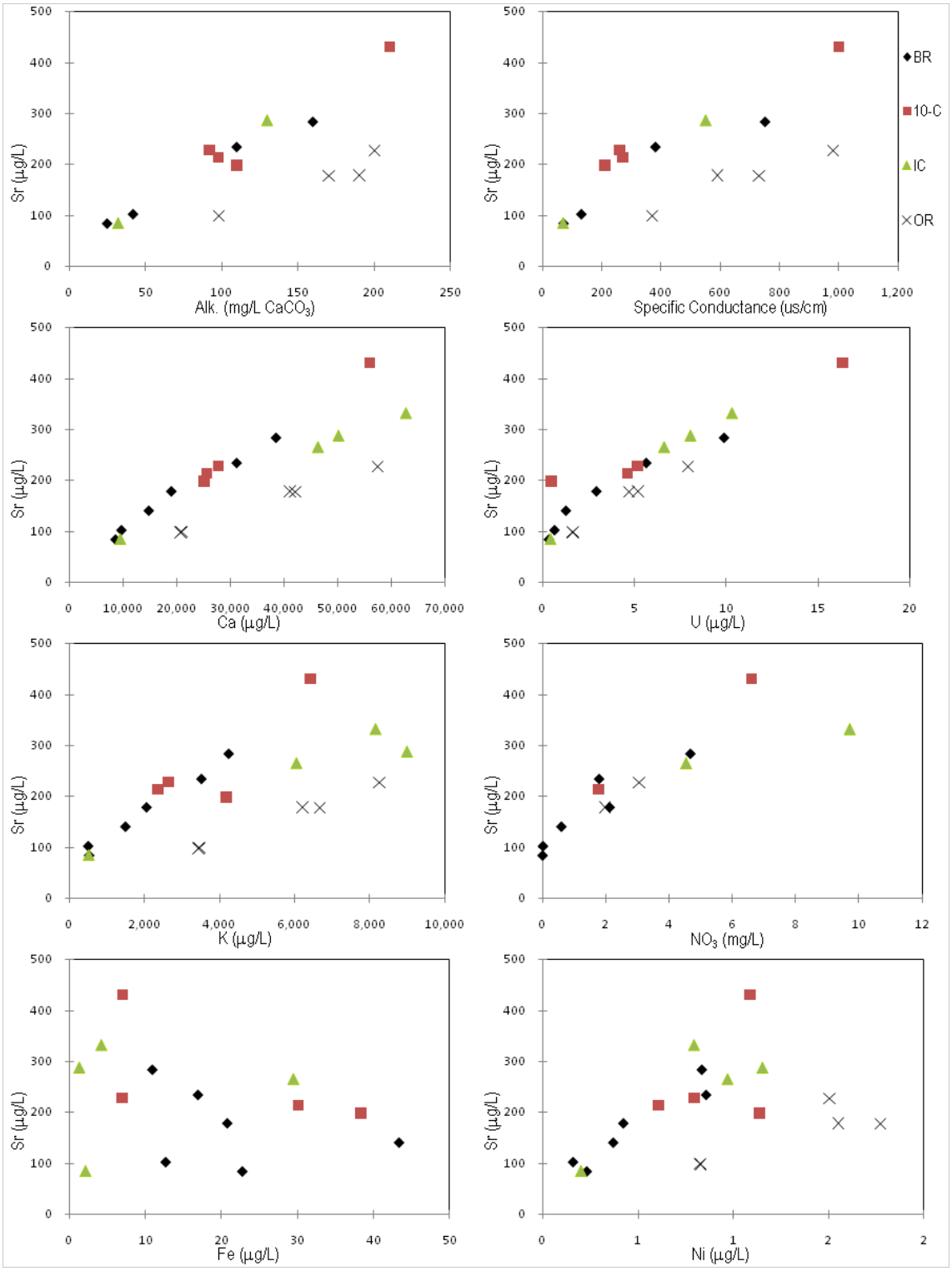

Figure 6: Surface water strontium concentrations plotted against other dissolved species and parameters. Data is plotted for synoptic sampling of: Boise River (BR), 10-Mile Ck. (10-C), Indian Ck. (IC), and Owyhee River (OR). Owyhee River samples are omitted from one plot to allow for focusing on the scale of the Boise River and its tributaries.

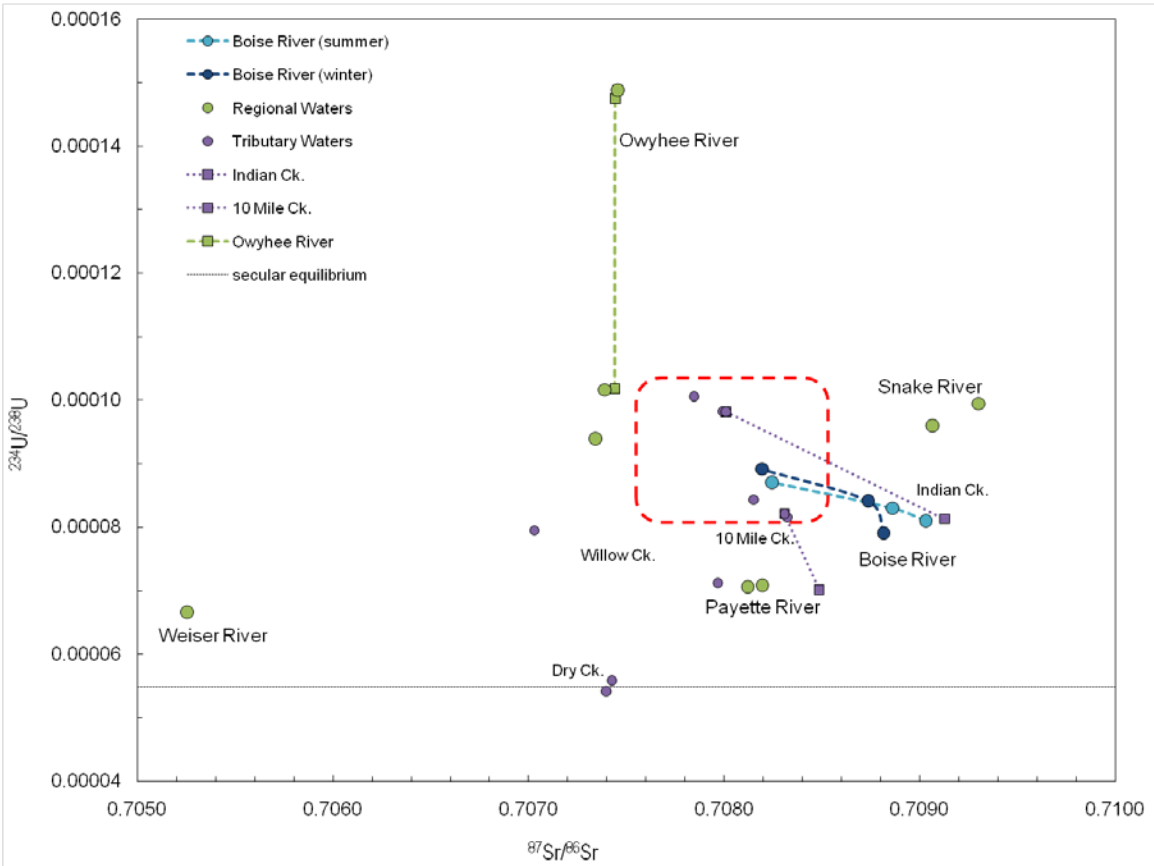

Figure 7: Boise River Watershed and regional river isotopic compositions. Dashed lines indicate surface waters evolving downstream toward the nexus of convergence depicted as a dashed rectangle near the center of the plot.

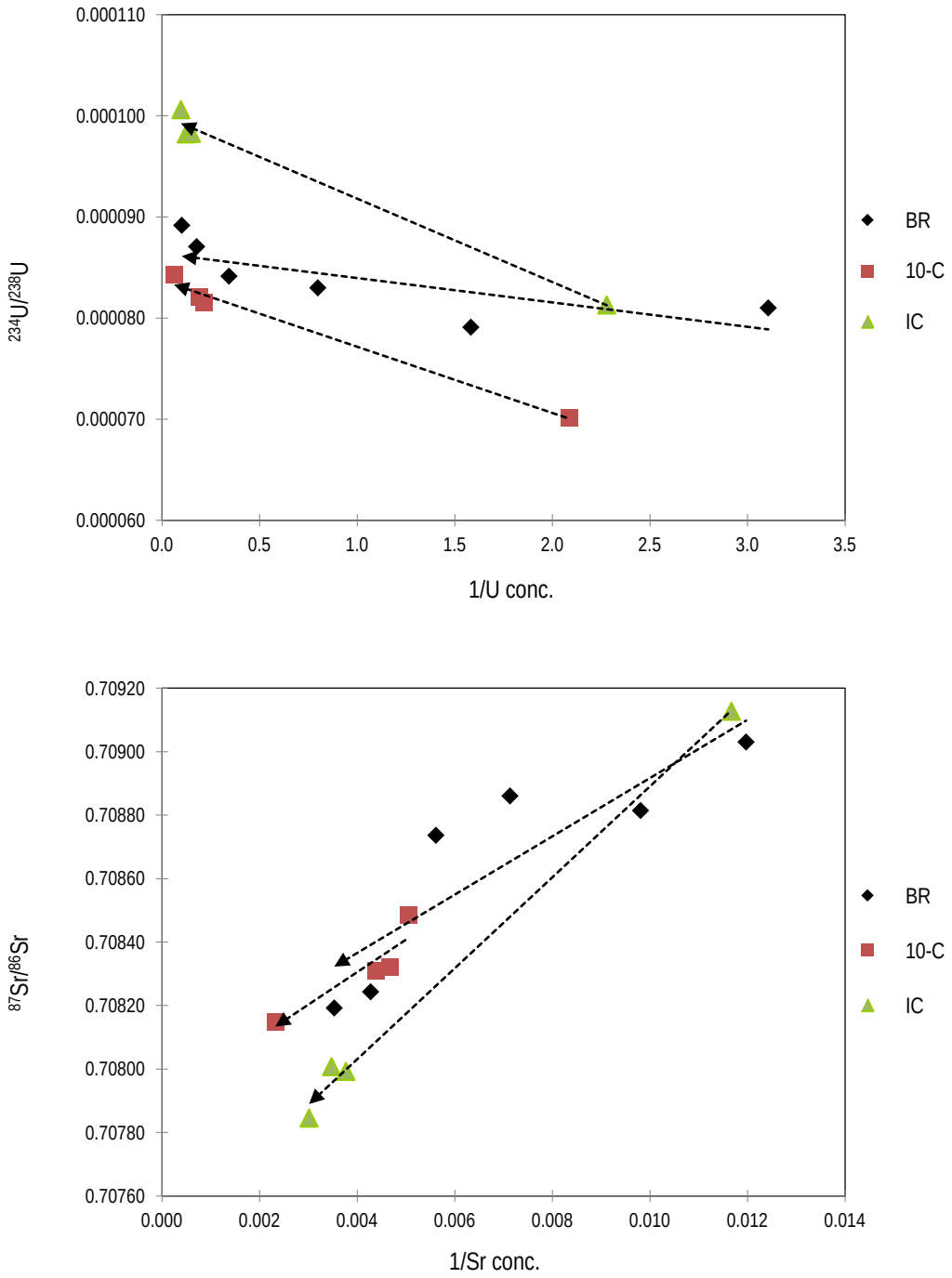

Figure 8: Surface water isotopic mixing displayed in both $^{234}U/^{238}U$ vs 1/U concentration (above) and $^{87}Sr/^{86}Sr$ vs 1/Sr concentration (below). Data is plotted for all samplings of: Boise River (BR), 10-Mile Ck. (10-C), and Indian Ck. (IC). Mixing arrays are made linear in reciprocal concentration space. The approximate linearity of the arrays suggests that surface waters are predominantly experiencing two component mixing with respect to U and Sr.

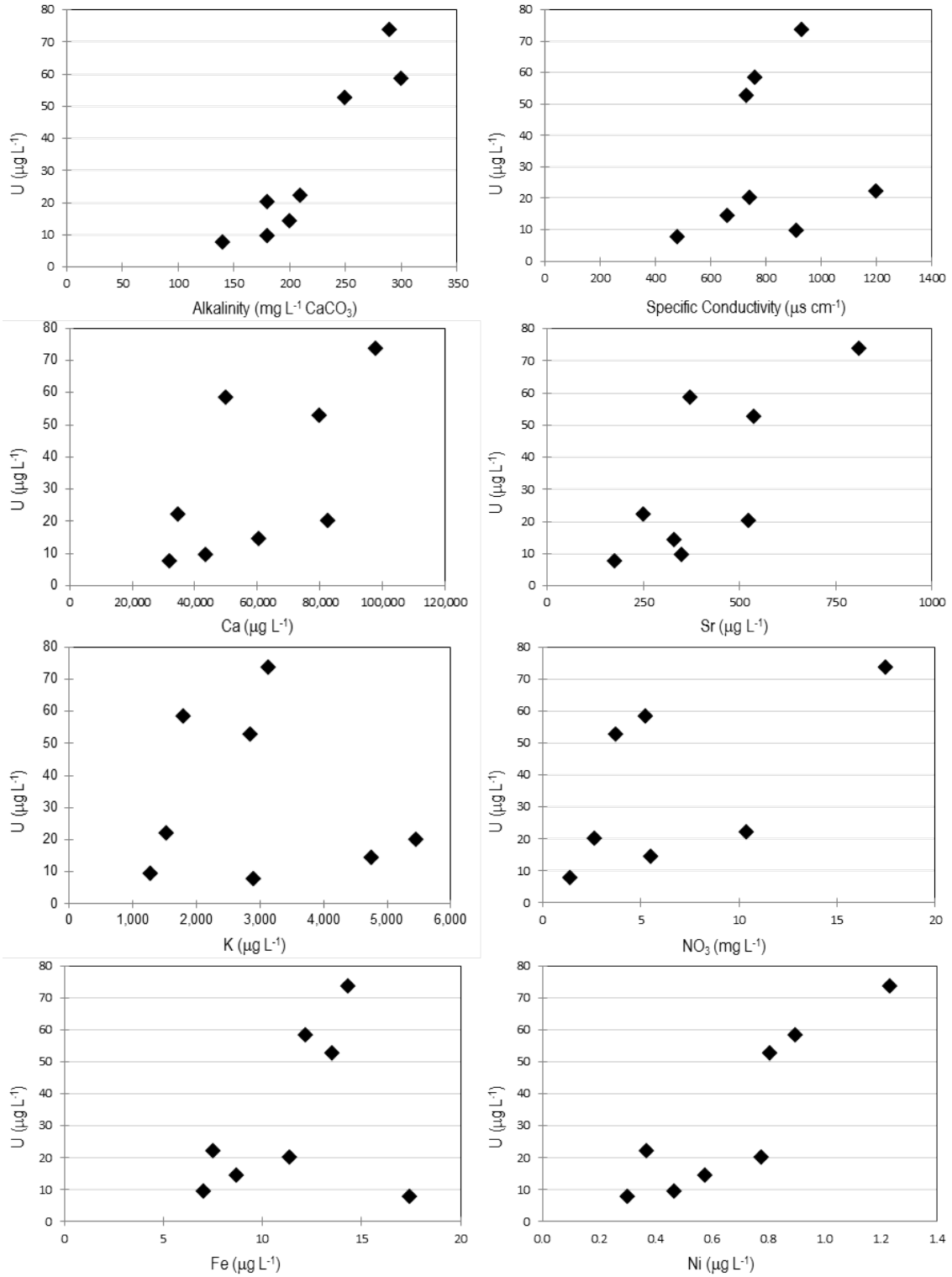

Figure 9: Groundwater uranium concentrations plotted against other dissolved species and parameters for the eight wells sampled during this study.

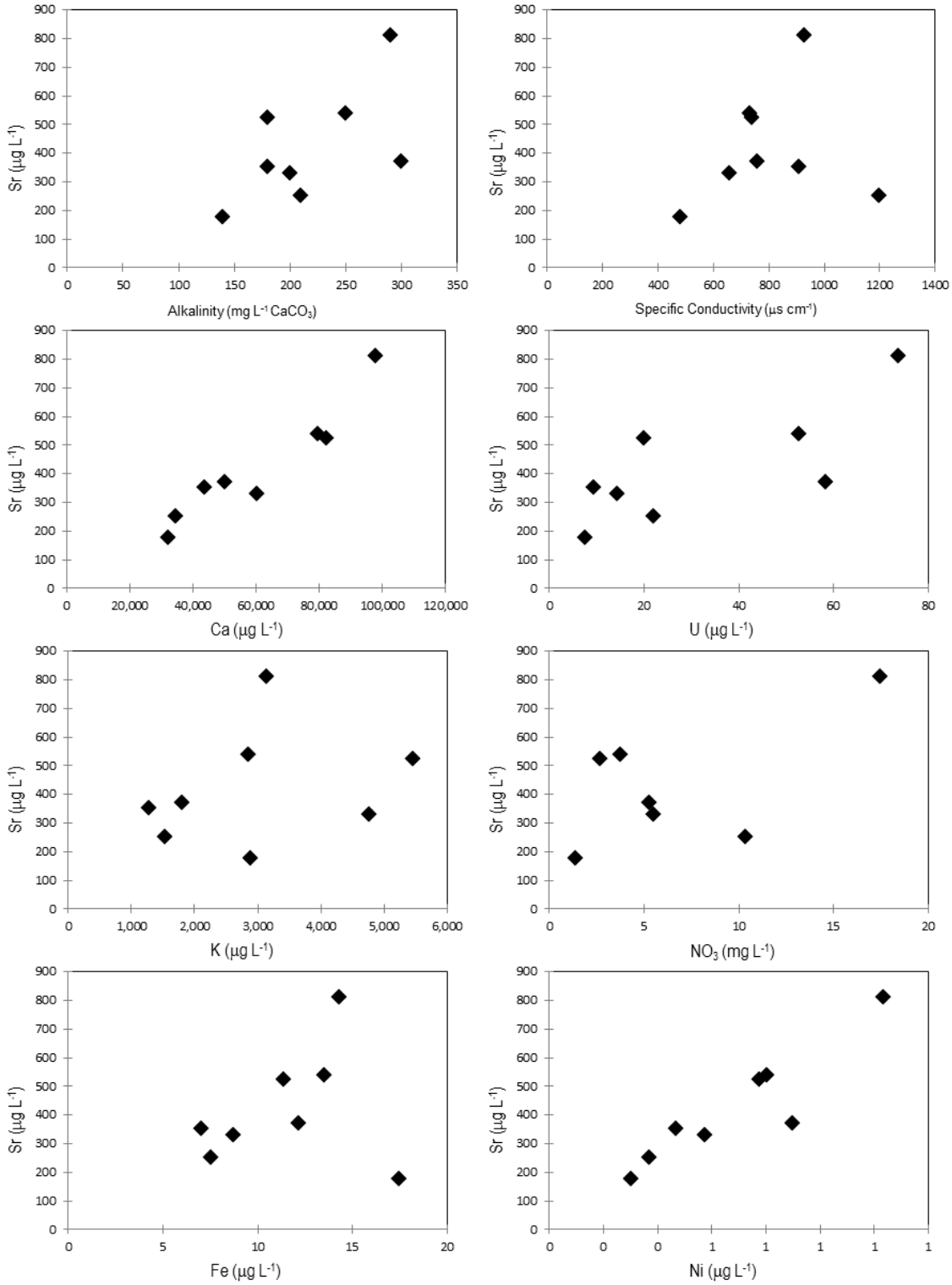

Figure 10: Groundwater strontium concentrations plotted against other dissolved species and parameters for the eight wells sampled during this study.

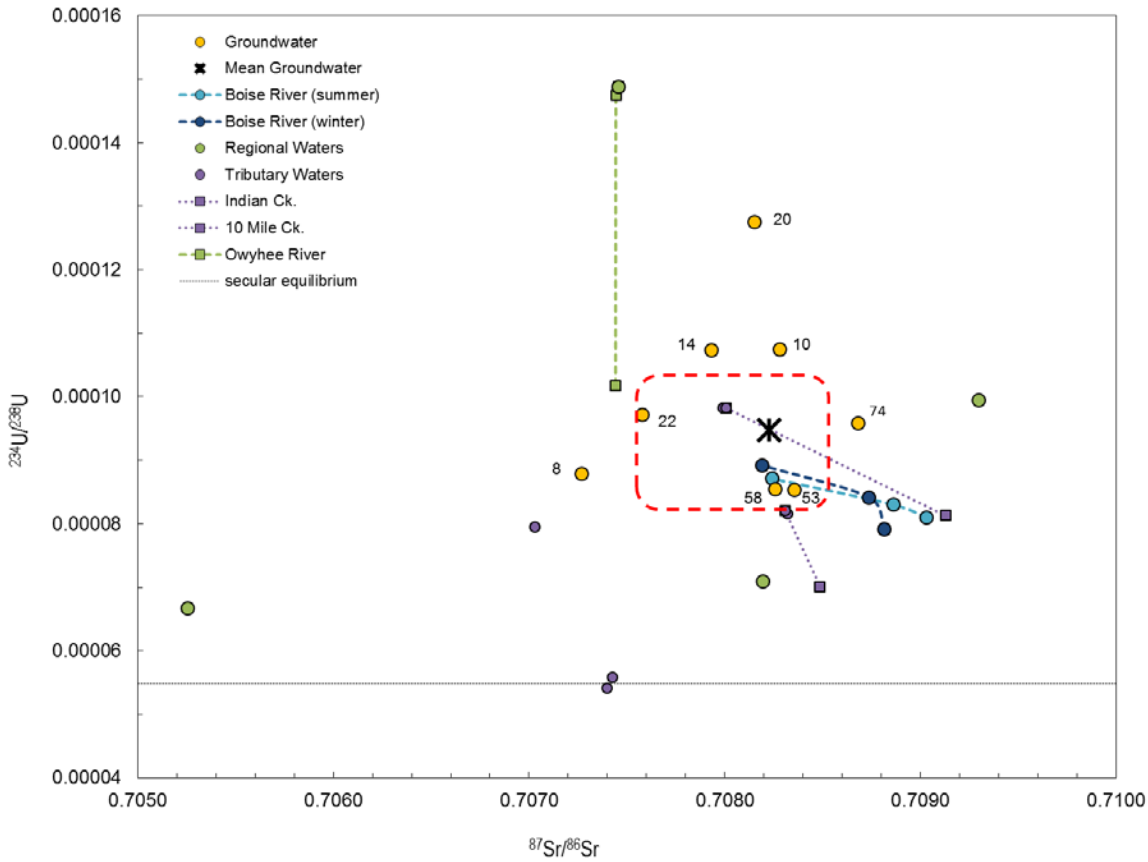

Figure 11: Treasure Valley groundwater isotopic compositions from eight wells sampled for this study, as well as an estimate of mean weighted "average" groundwater isotopic composition. Uranium concentrations of each well are noted in units of μg L^{-1}.

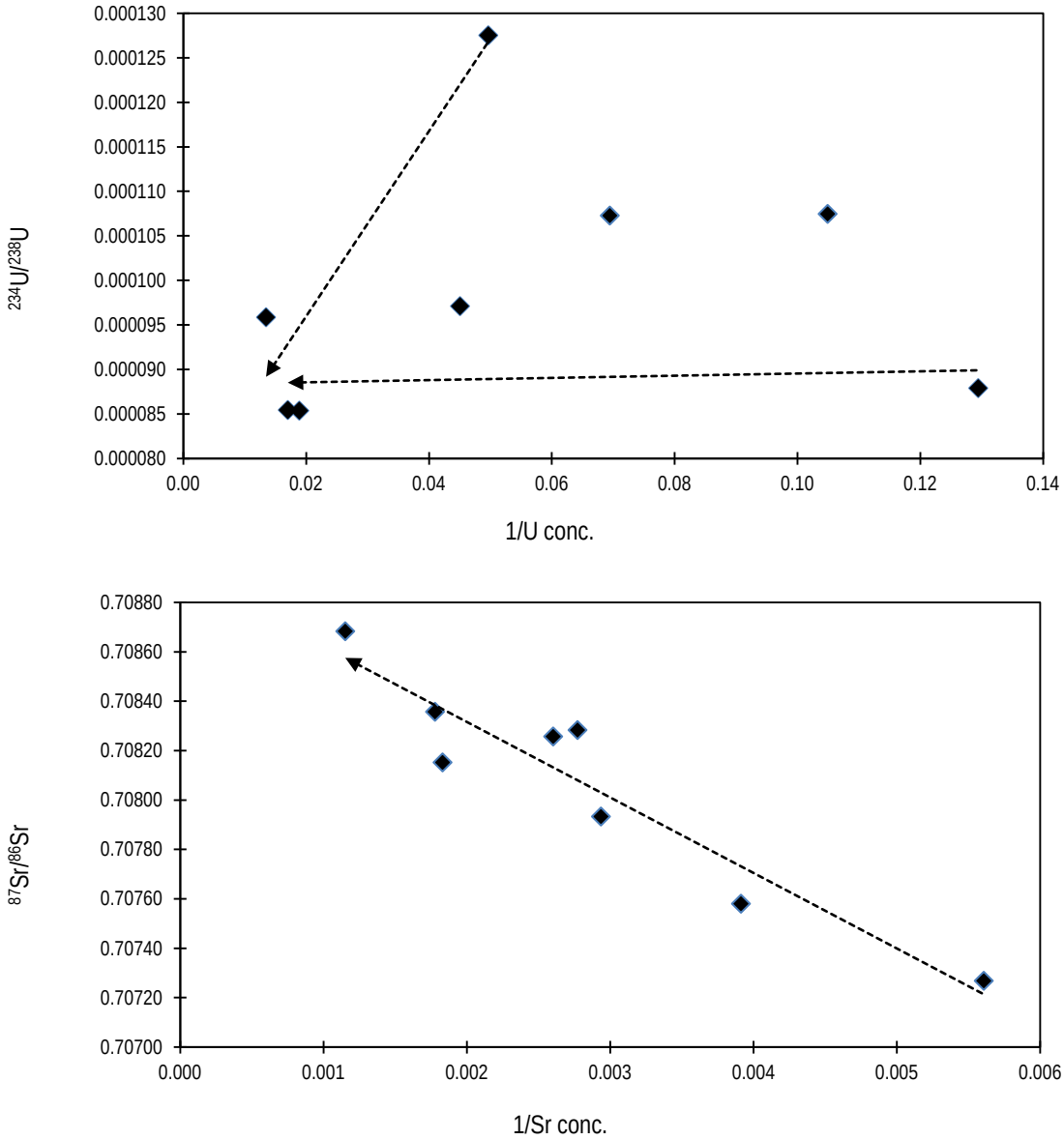

Figure 12: Groundwater isotopic mixing displayed in both $^{234}U/^{238}U$ vs 1/U concentration (above) and $^{87}Sr/^{86}Sr$ vs 1/Sr concentration (below). Well samples with higher U contents (low 1/U) have a smaller spread in $^{234}U/^{238}U$, suggesting a common U source. By comparison, lower U samples have diverse $^{234}U/^{238}U$ ratios from different sources. Unlike the multi-component scenario seen in the U data, two component mixing appears to be dominate with respect to Sr.

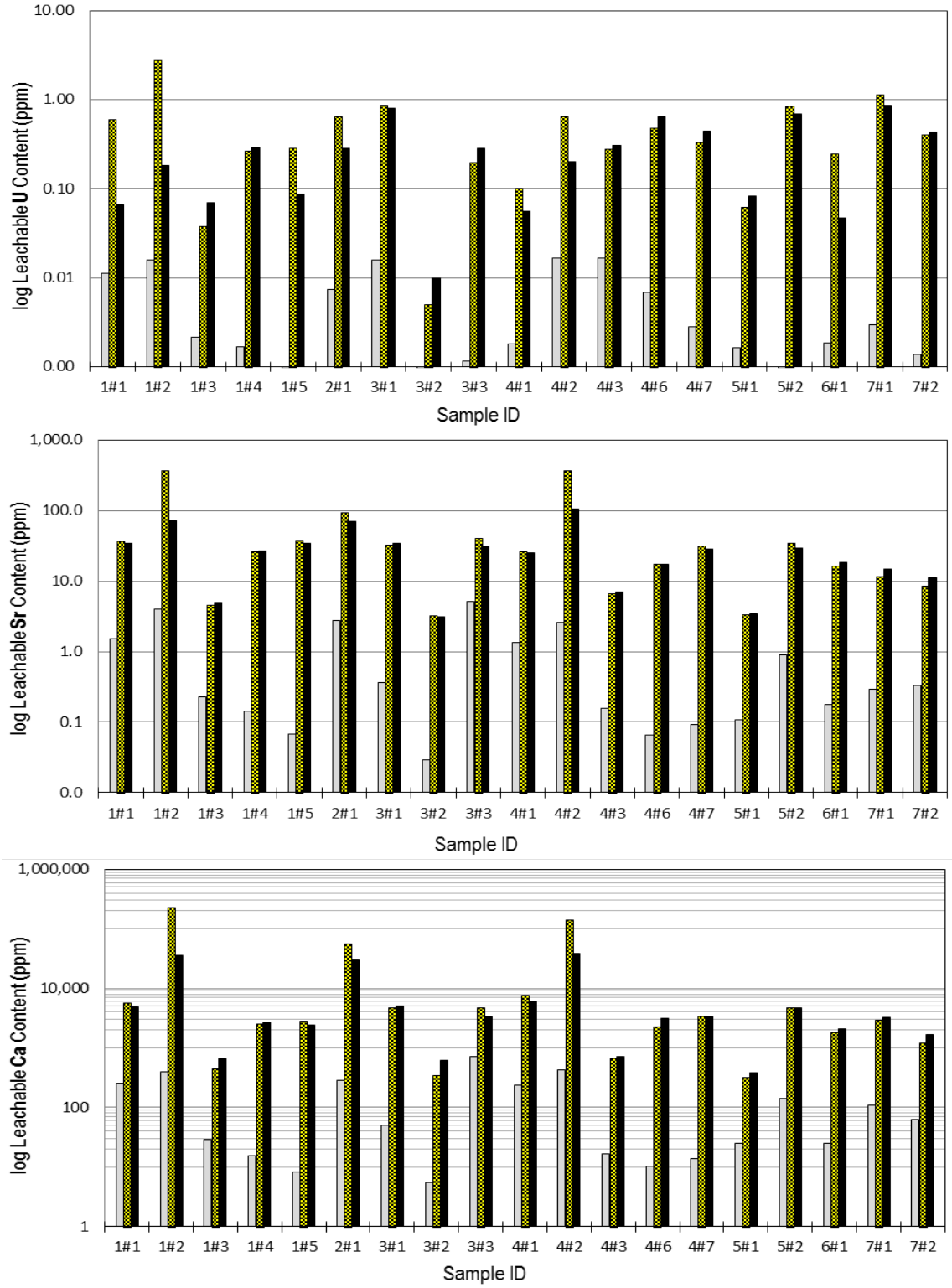

Figure 13: Bar graphs showing each solids sample's leachable contents of several elements from the three selective extraction treatments. Selective extractions are (left to right): DI water soluble (light), Carbonate (checkered), and oxide (dark).

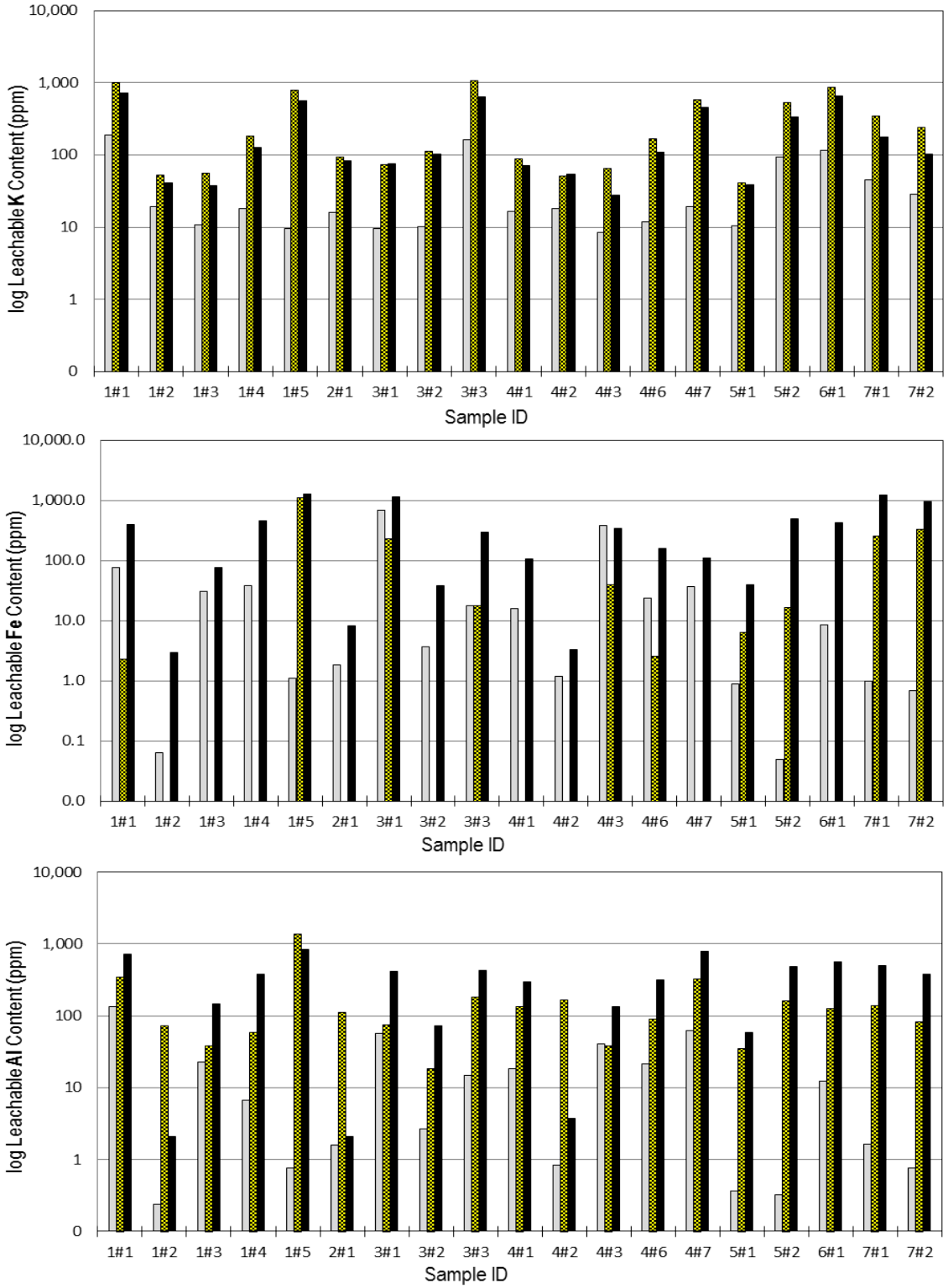

Figure 13: (continued) Bar graphs showing each solids sample's leachable contents of several elements from the three selective extraction treatments. Selective extractions are (left to right): DI water soluble (light), Carbonate (checkered), and oxide (dark).

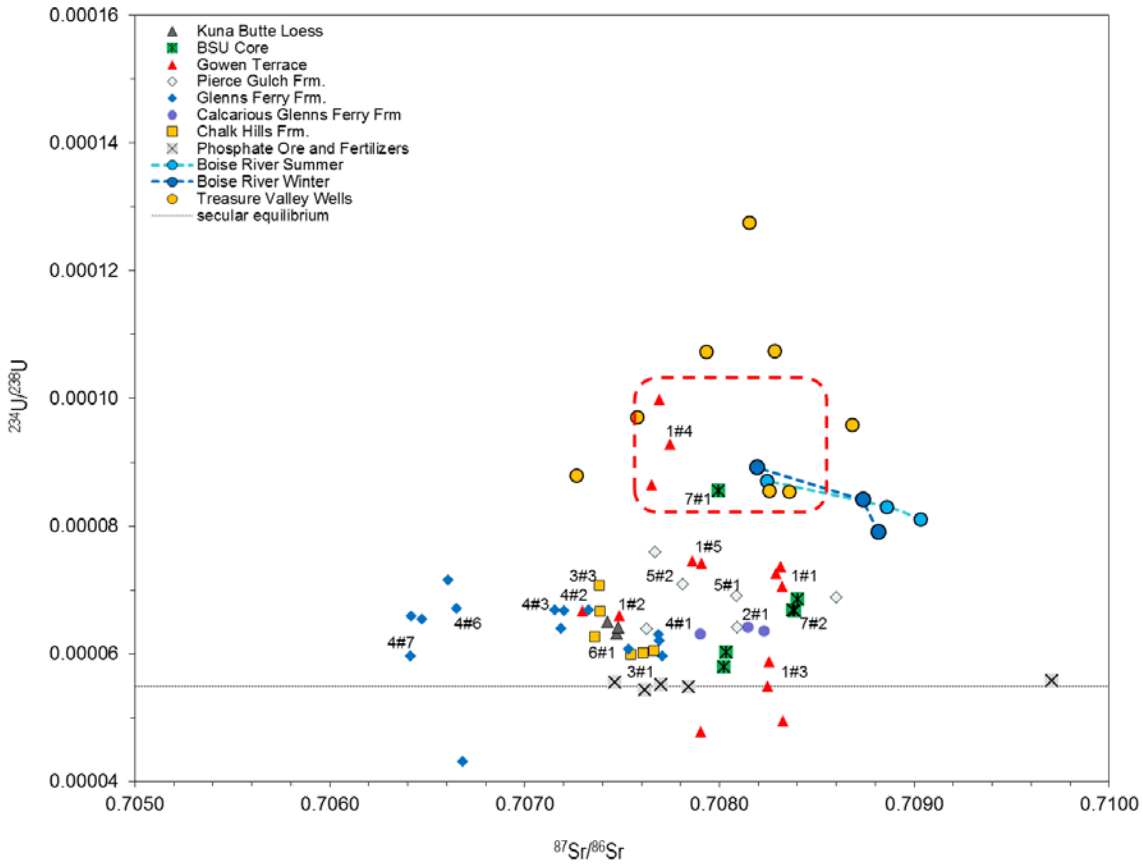

Figure 14: Isotopic compositions for leachates of the three extractions of each solid sample and total dissolutions of fertilizer and phosphate ore samples.

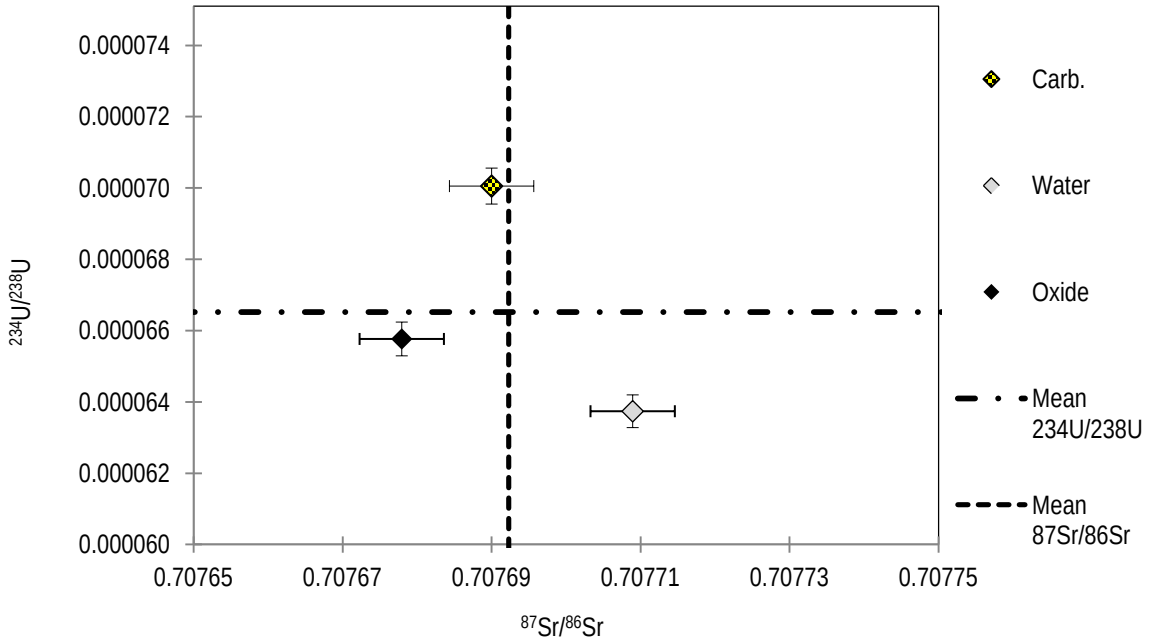

Figure 15: Plot of average isotopic compositions for each extraction scenario compared to the overall average for all scenarios combined. Error bars show the highest ± 1 sigma % error from all samples.

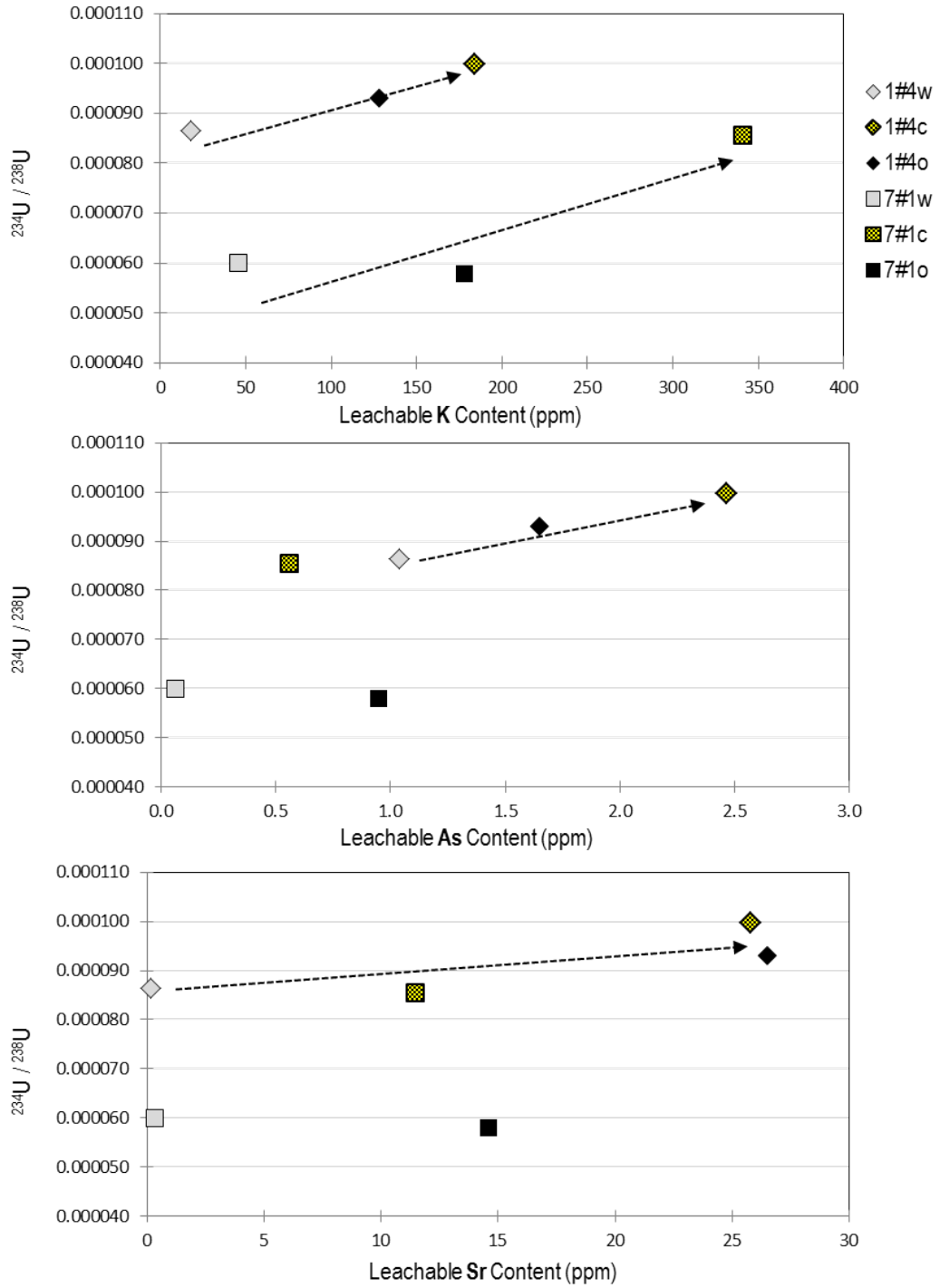

Figure 16: Plot showing a trend of increasing $^{234}U/^{238}U$ ratios in approximate correlation with increasing leachable K content for the three extractions of samples 1#4 and 7#1, and with As for sample 1#4. A weaker trend may also be present between $^{234}U/^{238}U$ and Sr for sample 1#4.

Table 1: Uranium Statistics for Public vs Private Well Data

	Mean U μg L^{-1}	**Median U μg L^{-1}**	**Max U μg L^{-1}**
Public Wells	18	12	95
Private Wells	33	26	110

Typical range of U concentrations in groundwater affected by natural U source: 0.1 – 100 μg L^{-1} (Langmuir, 1997. *Aqueous Environmental Geochemistry*).

Table 2: Surface Water Sample Details

	Sample ID	Max U Conc. $\mu g\ L^{-1}$	Number of Samples	Data Available
Upstream Boise River	**BR#1**	0.6	2	Anion, Cation, Field, Isotope
Mid Boise River	**BR#2**	2.9	2	Anion, Cation, Isotope
Downstream Boise River	**BR#3**	9.9	2	Anion, Cation, Field, Isotope
Dry Creek	**DC#1**	2.9	2	Anion, Cation, Isotope
Willow Creek	**WC#1**	1.4	2	Anion, Cation, Field, Isotope
Upstream 10 Mile Creek	**10C#1**	0.5	1	Cation, Field, Isotope
Downstream 10 Mile Creek	**10C#2**	16.4	3	Anion, Cation, Field, Isotope
Upstream Indian Creek	**IC#1**	0.4	1	Cation, Field, Isotope
Downstream Indian Creek	**IC#2**	10.3	3	Anion, Cation, Field, Isotope
Payette River	**PR#1**	0.9	2	Anion, Cation, Field, Isotope
Snake River	**SR#1**	3.8	2	Anion, Cation, Field, Isotope
Weiser River	**WR#1**	0.1	2	Anion, Cation, Field, Isotope
Upstream Owyhee River	**OR#1**	1.7	1	Cation, Field, Isotope
Mid Owyhee River	**OR#2**	1.7	1	Cation, Isotope
Downstream Owyhee River	**OR#3**	7.9	3	Anion, Cation, Field, Isotope

Full surface water data is available in appendix. Differentiating between repeated sampling events is accomplished by using letters following the sample ID. Surface waters were sampled: (a) Sept. 2009, (b) Feb. 2010, and (c) Sept. 2010.

Table 3: Groundwater Sample Details

	Sample ID	U Conc. $\mu g\ L^{-1}$	Well Type	Data Available
Northern Nampa	**W#1I**	9.5	Private	Cation, Field, Isotope
South of Meridian	**W#2I**	22.2	Private	Anion, Cation, Field, Isotope
Southern Meridian	**W#3I**	58.5	Private	Anion, Cation, Field, Isotope
North of Notus	**W#4I**	7.7	Private	Anion, Cation, Field, Isotope
North of Nampa	**W#5I**	73.8	Private	Anion, Cation, Field, Isotope
Kuna	**W#1Q**	20.1	Public	Anion, Cation, Field, Isotope
Southern Nampa	**W#2Q**	14.4	Public	Anion, Cation, Field, Isotope
South of Meridian	**W#3Q**	52.7	Public	Anion, Cation, Field, Isotope

Full groundwater data is available in appendix.

Table 4: Total Uranium Content of Solids and Phosphate Samples

	Sample ID	Formation	U Conc. (ppm)
Topsoil	**1#1**	Gowen Terrace	4.0
Carbonate-rich horizon	**1#2**	Gowen Terrace	7.0
Coarse sand	**1#3**	Gowen Terrace	2.3
Fe Oxide stained silty clay	**1#4**	Gowen Terrace	3.7
Gray silty clay	**1#5**	Gowen Terrace	3.6
Silt	**2#1**	Calcareous Glenns Ferry	4.4
Fe Oxide-rich sand	**3#1**	Chalk Hills	4.5
Ash	**3#2**	Chalk Hills	3.0
Silt / clay	**3#3**	Chalk Hills	3.3
Loess	**4#1**	Glenns Ferry	3.0
Carbonate-rich horizon	**4#2**	Glenns Ferry	2.9
Fe Oxide-rich sand	**4#3**	Glenns Ferry	1.2
Silt	**4#6**	Glenns Ferry	5.7
Ash	**4#7**	Glenns Ferry	3.0
Coarse Sand	**5#1**	Pierce Gulch	0.9
Silt	**5#2**	Pierce Gulch	5.0
Loess	**6#1**	Kuna Butte	3.4
Silt	**7#1**	Floodplain	n/a
Sandy Silt	**7#2**	Floodplain	n/a
Phosphate Ore (weathered)		Phosphoria	76
Phosphate Ore (unaltered)		Phosphoria	225
Fertilizer S			38
Fertilizer L			271
Fertilizer H			319

Wanty and Nordstrom (1995) provide estimates of average uranium content in geologic solids: 2.7 ppm for all crustal materials and 4.4 ppm for granitic materials.

Table 5: Total Dissolution and Selective Extraction Results

		Water	Carbonate	Fe/Mn Oxide	Total Dissolution
		ppb	ppb	ppb	ppb
River Terrace					
Topsoil	1#1	11.1	586.7	66.0	4000
Carbonate-rich Horizon	1#2	16.0	2,740.4	180.3	7000
Coarse Sand	1#3	2.2	37.5	69.2	2300
Fe Oxide Clay/Silt	1#4	1.7	262.3	288.7	3700
Gray Clay/Silt	1#5	0.5	283.0	87.7	3600
Calcarioius Glenns Ferrry					
Silt	2#1	7.5	639.3	286.8	4400
Chalk Hills					
Fe Oxide Sands	3#1	15.8	862.0	803.4	4500
Ash	3#2	0.1	5.0	10.0	3000
Silt/Clay	3#3	1.2	196.5	284.0	3300
Non-Calc. Glenns Ferry					
Loess	4#1	1.8	101.1	56.2	3000
Carbonate-rich Horizon	4#2	16.9	644.9	202.3	2900
Fe Oxide Sands	4#3	16.5	276.9	307.0	1200
Silt	4#6	6.8	476.0	649.6	5700
Ash	4#7	2.8	328.1	446.3	3000
Pierce Gulch					
Coarse Sand	5#1	1.6	60.8	82.2	900
Silt	5#2	0.9	833.5	697.4	5000
Kuna Butte					
Loess	6#1	1.8	241.2	46.7	3430
Floodplain Core					
Silt	7#1	2.9	1,124.2	869.5	
Silt/Sand	7#2	1.4	403.4	436.9	

Total uranium contents and leachable uranium contents from each of the three selective extractions treatments.

APPENDIX A

Complete Geochemical Data for Surface Water Samples

Complete Geochemical Data for Surface Water Samples (page 1)

		anlytical instrument	detection limit	instrument accuracy (+/-)	instrument precision (+/-)	blank	BR#1 a	BR#1 b	BR#2 a	BR#2 b	BR#3 a	BR#3 b	NYC#1 a	DC#1 a	DC#1 b	WC#1 a	WC#1 b
$^{234}U/^{238}U$		TI-MS					0.0000810	0.0000791	0.0000830	0.0000841	0.0000871	0.0000892	0.0000811	0.0000559	0.0000541	0.0000712	0.0000795
$[^{234}U/^{238}U]$		TI-MS					1.48	1.44	1.51	1.53	1.59	1.62	1.48	1.02	0.986	1.30	1.45
$^{87}Sr/^{86}Sr$		TI-MS					0.70903	0.70882	0.70886	0.70874	0.70824	0.70819	0.70895	0.70743	0.70740	0.70797	0.70703
Na	(µg/L)	ICP-MS	5	7.4%	1.3%	0.104	3,159	4,048	11,480	18,110	31,120	44,270	3,537	8,028	7,547	4,461	14,440
Mg	(µg/L)	ICP-MS	1	6.5%	1.4%	0.479	906.8	1,133	2,243	3,209	8,489	11,420	1,281	2,353	1,993	1,099	5,553
Si	(µg/L)	ICP-MS	10	11.7%	1.4%	10.1	4,955	5,444	5,589	5,277	10,680	12,630	5,389	12,430	11,380	4,275	10,200
K	(µg/L)	ICP-MS	5	13.3%	1.3%	5.22	538.7	514.0	1,504	2,066	3,525	4,252	529.0	1,557	968.9	833.5	3,672
Ca	(µg/L)	ICP-MS	5	8.0%	1.2%	3.35	8,654	9,749	14,850	19,050	31,240	38,570	9,747	22,710	20,210	7,056	22,160
Sr	(µg/L)	ICP-MS	0.05	3.6%	1.0%	0.023	83.55	102.0	140.2	178.2	233.9	283.4	89.59	277.2	252.6	84.88	213.9
Ba	(µg/L)	ICP-MS	0.5	9.0%	1.0%	0.033	8.822	11.81	16.16	23.57	40.14	47.91	9.526	44.87	37.27	16.52	62.61
U	(µg/L)	ICP-MS	0.01	2.2%	1.6%	0.013	0.322	0.632	1.253	2.916	5.637	9.884	0.362	1.864	2.854	0.138	1.425
Cr	(µg/L)	ICP-MS	0.05	3.2%	5.3%	0.041	0.006	0.104	0.011	0.212	0.167	0.658	0.005	0.032	0.190	0.000	0.368
Mn	(µg/L)	ICP-MS	1	3.2%	2.3%	0.057	1.121	0.541	27.16	30.28	14.08	22.87	3.079	4.910	1.616	9.623	22.13
Fe	(µg/L)	ICP-MS	5	6.6%	10.3%	0.000	22.75	12.71	43.29	20.78	16.94	10.97	20.56	44.57	18.13	34.90	161.4
Ni	(µg/L)	ICP-MS	0.01	2.4%	7.2%	0.000	0.229	0.157	0.368	0.421	0.856	0.833	0.151	0.349	0.238	0.172	1.506
Cu	(µg/L)	ICP-MS	0.05	2.5%	12.1%	0.019	0.566	0.071	0.566	0.674	0.794	0.536	0.550	0.000	0.000	1.509	4.615
Zn	(µg/L)	ICP-MS	0.05	1.6%	5.4%	0.203	21.76	0.140	3.548	5.283	1.997	2.777	0.245	0.759	0.255	1.252	2.577
Cd	(µg/L)	ICP-MS	0.05	2.3%	25.8%	0.012	0.000	0.007	0.000	0.007	0.006	0.030	0.000	0.025	0.022	0.000	0.126
Pb	(µg/L)	ICP-MS	0.01	1.9%	12.6%	0.010	0.000	0.011	0.000	0.041	0.006	0.072	0.000	0.020	0.020	0.000	0.236
Al	(µg/L)	ICP-MS	1	11.5%	4.9%	0.336	17.66	13.09	1.863	1.350	3.321	1.590	14.69	3.197	20.78	7.485	180.3
P	(µg/L)	ICP-MS	10	11.8%	7.1%	2.83	16.75	0.000	241.1	397.5	252.5	358.1	11.85	52.66	21.54	22.72	90.75
As	(µg/L)	ICP-MS	0.05	2.4%	12.0%	0.144	2.201	2.202	3.094	2.292	6.480	6.901	2.767	3.947	1.627	4.112	48.78
Se	(µg/L)	ICP-MS	0.5	28.6%	32.0%	0.000	0.000	0.000	0.000	0.000	0.241	0.589	0.374	0.033	0.163	0.323	0.420
Br	(mg/L)	IC	0.025	12.0%	4.9%	0.003	0.000	0.007	0.011	0.035	0.042	0.074	0.000	0.000	0.007	0.005	0.015
Cl	(mg/L)	IC	0.25	7.3%	4.5%	0.125	0.554	0.600	5.73	12.2	11.9	21.8	0.467	0.935	2.06	0.692	4.42
F	(mg/L)	IC	0.025	4.0%	8.4%	0.022	0.237	0.316	0.314	0.426	0.386	0.471	0.242	0.109	0.109	0.347	0.290
NO_3	(mg/L)	IC	0.025	5.2%	1.1%	0.020	0.012	0.025	0.603	2.12	1.790	4.66	0.059	0.012	0.218	0.000	0.217
NO_2	(mg/L)	IC	0.05	12.8%	13.6%	0.011	0.000	0.015	0.000	0.000	0.000	0.007	0.000	0.000	0.004	0.000	0.002
PO_4	(mg/L)	IC	0.025	6.0%	5.8%	0.000	0.007	0.000	0.197	0.316	0.182	0.279	0.007	0.035	0.016	0.008	0.067
SO_4	(mg/L)	IC	0.5	12.0%	5.6%	0.167	1.74	2.20	6.88	11.1	27.3	41.7	2.17	1.59	2.43	1.30	30.7
Alkalinity	(mg/L $CaCO_3$)	field kit		15%	15%		25	42			110	160	38			32	75
pH	std. unit	multi-meter		0.1 std. unit	0.05 std. unit		7.6	7.7			8.3	8.1	8.2			7.5	7.8
DO	(mg/L)	multi-meter		1.5 mg/L	1.0 mg/L		7.3	14			13	14	11			9.3	16
ORP	(mV)	multi-meter		25%	15%		19	-73			-12	-94	-23			-1.5	-99
Spec. Cond	(µS/cm)	multi-meter		15%	5%		70	130			380	750	80			69	360

Uncertainty (+/- 1σ) associated with isotopic data generated by TI-MS analysis is less than 0.56% for all $^{234}U/^{238}U$ samples and less than 0.0008% for all $^{87}Sr/^{86}Sr$ samples.

Analytical instruments/methods used include: (TI-MS) multi-collector thermal ionization mass spectrometry, (ICP-MS) inductively coupled plasma mass spectrometry, (IC) ion chromatography, (multi-meter) handheld field water chemistry meter, and (field kit) colormetric alkalinity kit.

Complete Geochemical Data for Surface Water Samples (page 2)

	10C#1 c	10C#2 c	10C#2 b	10C#2 a	IC#1 c	IC#2 c	IC#2 b	IC#2 a	PR#1 a	PR# 1 b	SR#1 a	SR#1 b	WR#1 a	WR#1 b	OR#1 c	OR#2 c	OR#3 c	OR#3 b	OR#3 a
$^{234}U/^{238}U$	0.0000701	0.0000821	0.0000843	0.0000816	0.0000813	0.0000982	0.000101	0.0000983	0.0000709	0.0000706	0.0000960	0.0000995	0.0000666		0.000149	0.000148	0.000102	0.0000939	0.000102
$[^{234}U/^{238}U]$	1.28	1.50	1.54	1.49	1.48	1.79	1.83	1.79	1.29	1.29	1.75	1.81	1.21		2.71	2.69	1.85	1.71	1.85
$^{87}Sr/^{86}Sr$	0.70849	0.70831	0.70815	0.70832	0.70913	0.70801	0.70785	0.70799	0.70820	0.70812	0.70906	0.70930	0.70525	0.70493	0.70746	0.70744	0.70744	0.70734	0.70739
Na	13,640	18,180	65,340	17,630	3,308	52,150	64,430	43,930	3,867	6,721	32,450	30,330	9,117	6,955	28,970	29,530	61,110	100,400	66,680
Mg	5,670	7,502	17,660	6,986	1,002	15,780	20,380	13,780	777.5	1,186	18,430	19,230	5,626	4,759	5,545	5,532	10,700	15,870	11,190
Si	12,670	11,200	15,530	10,560	5,411	20,330	20,460	17,760	4,764	6,646	9,216	13,600	15,840	11,640	6,705	5,672	15,250	15,060	13,420
K	4,185	2,638	6,429	2,364	509.8	8,987	8,150	6,043	666.5	778.3	4,755	4,680	3,290	1,881	3,468	3,437	6,675	8,259	6,209
Ca	25,160	27,800	56,000	25,610	9,509	50,170	62,740	46,350	6,158	10,500	44,640	48,090	13,150	11,370	20,940	20,750	42,110	57,540	41,150
Sr	198.3	228.4	430.9	213.6	85.71	287.9	331.8	265.3	78.95	132.1	266.1	274.5	74.87	56.42	99.84	98.23	178.0	227.2	178.5
Ba	52.89	44.65	69.88	39.40	8.895	61.85	67.12	55.68	10.87	14.57	42.11	42.16	49.01	10.76	16.21	15.57	32.92	28.04	28.25
U	0.479	5.176	16.35	4.612	0.439	8.059	10.32	6.626	0.286	0.901	3.838	3.495	0.133	0.123	1.653	1.652	4.720	7.905	5.193
Cr	0.912	0.887	0.555	0.091	0.238	2.255	1.256	0.495	0.000	0.193	0.589	1.389	0.544	0.208	0.890	0.773	1.611	1.035	0.259
Mn	26.23	6.580	23.63	6.813	3.339	7.507	17.69	9.439	8.286	11.993	8.615	5.707	12.31	21.38	0.951	3.874	55.76	52.40	38.75
Fe	38.34	6.935	6.978	30.08	2.112	1.301	4.194	29.39	23.17	38.22	10.88	1.078	1,117	59.14	18.04	14.82	264.4	78.34	31.40
Ni	1.138	0.794	1.088	0.607	0.200	1.152	0.793	0.969	0.069	0.102	0.849	0.642	1.403	0.505	0.825	0.829	1.770	1.504	1.550
Cu	0.914	1.380	1.544	2.415	0.547	1.247	0.388	0.798	0.000	0.000	0.339	0.333	2.698	0.758	0.852	0.742	1.349	0.743	0.587
Zn	2.658	1.696	12.86	2.798	1.649	4.530	2.202	2.470	0.928	0.327	1.626	0.184	8.283	0.007	1.751	0.730	1.777	0.516	1.610
Cd	0.000	0.001	0.019	0.000	0.000	0.000	0.007	0.000	0.000	0.028	0.025	0.022	0.021	0.029	0.000	0.000	0.016	0.079	0.000
Pb	0.008	0.016	0.076	0.006	0.004	0.032	0.018	0.040	0.000	0.018	0.036	0.049	0.186	0.042	0.020	0.019	0.272	0.131	0.000
Al	5.631	6.055	1.740	14.01	2.620	3.684	2.560	24.54	4.912	18.01	3.026	1.220	1,067	6.230	42.96	32.44	270.2	77.02	30.30
P	129.2	202.6	972.0	243.5	0.000	622.5	693.9	568.8	7.302	11.73	50.72	41.35	102.6	9.108	0.000	0.000	63.00	76.08	54.55
As	2.356	4.111	4.548	4.131	2.046	8.338	8.618	7.642	0.313	0.117	6.706	4.598	2.047	1.117	6.615	6.759	24.83	36.62	26.48
Se	0.000	0.000	1.746	0.201	0.000	0.168	2.940	0.753	0.000	2.314	1.319	1.179	0.092	0.001	0.000	0.000	1.411	5.470	2.063
Br			0.084	0.026			0.124	0.082	0.006	0.011	0.049	0.061	0.007	0.007				0.102	0.071
Cl			51.1	6.43			28.2	19.2	0.604	1.25	23.7	27.2	1.31	2.16				21.3	15.6
F			0.470	0.336			0.450	0.391	0.380	0.688	0.427	0.453	0.142	0.069				1.17	1.03
NO_3			6.60	1.770			9.71	4.540	0.000	0.023	1.12	1.70	0.002	0.004				3.04	1.96
NO_2			0.033	0.000			0.000	0.000	0.000	0.001	0.000	0.000	0.000	0.012				0.000	0.000
PO_4			0.710	0.183			0.472	0.414	0.002	0.000	0.014	0.007	0.053	0.000				0.014	0.014
SO_4			51.6	15.1			69.0	44.2	1.15	2.07	56.0	51.1	4.23	3.77				141	88.7
Alkalinity	110	92	210	98	32	130			27	34	170	170	75	59	98		170	200	190
pH	7.4	8.1	8.5	8.1	8.1	8.1			8.1	8.0	7.9	8.4	8.4	8.2	8.6		7.9	8.2	8.0
DO	7.5	11	15	11	10	10			11	14	9.3	14	11	16	12		9	13	11
ORP	-12	-16	-110	-14	-10	-14			-29	-27	-34	-89	-32	-85	-8.4		-12	-84	-37
Spec. Cond	210	260	1000	270	70	550			60	110	520	660	150	170	370		730	980	590

APPENDIX B

Complete Geochemical Data for Groundwater Samples

Complete Geochemical Data for Groundwater Samples

		anlytical instrument	detection limit	instrument accuracy (+/-)	instument precision (+/-)	blank	W#1I	W#2I	W#3I	W#4I	W#5I	W#1Q	W#2Q	W#3Q
$^{34}U/^{238}U$		TI-MS					0.000107	0.0000971	0.0000854	0.0000879	0.0000959	0.000128	0.000107	0.0000854
$^{234}U/^{238}U]$		TI-MS					1.96	1.77	1.56	1.60	1.75	2.32	1.95	1.56
$^{7}Sr/^{86}Sr$		TI-MS					0.70828	0.70758	0.70826	0.70727	0.70868	0.70815	0.70793	0.70836
Na	(µg/L)	ICP-MS	5	4.6%	0.7%	0.776	47,620	87,450	108,300	62,740	89,030	60,380	68,310	65,710
Mg	(µg/L)	ICP-MS	1	7.4%	0.8%	0.713	8,836	12,000	10,870	7,114	20,230	16,130	12,620	16,830
Si	(µg/L)	ICP-MS	10	17.6%	0.9%	13.5	17,330	17,550	12,600	17,200	16,640	18,210	18,600	17,310
K	(µg/L)	ICP-MS	5	7.6%	0.7%	7.71	1,290	1,528	1,805	2,897	3,144	5,457	4,759	2,853
Ca	(µg/L)	ICP-MS	5	7.6%	0.7%	3.35	43,710	34,690	50,030	32,060	97,860	82,400	60,390	79,680
Sr	(µg/L)	ICP-MS	0.05	3.9%	0.6%	0.156	350.5	250.4	372.7	175.8	811.4	523.2	331.5	538.0
Ba	(µg/L)	ICP-MS	0.5	1.9%	0.6%	0.068	73.35	64.87	58.22	32.71	49.35	80.86	45.27	69.11
U	(µg/L)	ICP-MS	0.01	3.5%	0.7%	0.108	9.524	22.15	58.47	7.721	73.75	20.10	14.38	52.70
Cr	(µg/L)	ICP-MS	0.05	2.2%	4.2%	0.085	0.222	0.331	0.867	0.992	0.532	1.622	1.233	0.589
Mn	(µg/L)	ICP-MS	1	4.2%	8.9%	0.376	0.000	0.000	1.033	0.187	0.422	0.000	0.000	1.049
Fe	(µg/L)	ICP-MS	5	4.5%	4.6%	0.000	7.039	7.544	12.19	17.45	14.33	11.39	8.717	13.54
Ni	(µg/L)	ICP-MS	0.01	1.1%	4.4%	0.031	0.468	0.370	0.899	0.304	1.234	0.778	0.577	0.806
Cu	(µg/L)	ICP-MS	0.05	4.8%	2.1%	0.522	3.916	1.025	2.478	0.000	7.395	0.609	1.578	30.77
Zn	(µg/L)	ICP-MS	0.05	11.1%	1.1%	0.203	4.302	54.61	43.67	15.23	5.014	4.654	3.248	12.82
Cd	(µg/L)	ICP-MS	0.05	0.9%	25.8%	0.061	0.000	0.036	0.376	0.000	0.000	0.015	0.000	0.000
Pb	(µg/L)	ICP-MS	0.01	1.7%	5.7%	0.083	0.112	0.490	0.546	0.001	0.064	0.168	0.051	0.125
Al	(µg/L)	ICP-MS	1	2.9%	8.2%	0.336	0.351	0.372	1.148	0.502	0.390	0.495	0.062	0.083
P	(µg/L)	ICP-MS	10	6.7%	3.4%	2.83	40.37	35.71	34.74	79.63	121.6	23.48	19.18	43.41
As	(µg/L)	ICP-MS	0.05	2.5%	3.5%	0.144	1.471	3.969	1.124	9.134	2.066	3.384	3.419	1.240
Se	(µg/L)	ICP-MS	0.5	6.6%	14.7%	0.000	0.456	0.870	1.016	1.188	1.916	2.263	1.854	1.638
Cl	(mg/L)	IC	0.025	12.0%	4.9%	0.011		0.057	0.044	0.110	0.114	0.251	0.110	0.096
I	(mg/L)	IC	0.25	9.9%	4.5%	0.549		15.6	15.4	18.8	21.6	30.1	15.1	9.3
F	(mg/L)	IC	0.025	12.4%	8.4%	0.014		0.510	0.666	0.551	0.271	0.085	0.436	0.198
NO_3	(mg/L)	IC	0.025	10.0%	1.1%	0.020		10.4	5.27	1.39	17.5	2.67	5.54	3.74
NO_2	(mg/L)	IC	0.05	12.8%	13.6%	0.018		0.000	0.000	0.000	0.000	0.000	0.000	0.000
PO_4	(mg/L)	IC	0.025	7.2%	5.8%	0.010		0.000	0.000	0.032	0.033	0.000	0.000	0.000
SO_4	(mg/L)	IC	0.5	12.0%	5.6%	0.516		37.3	47.6	57.4	116	150	88.4	86.8
Alkalinity	(mg/L $CaCO_3$)	field kit		15%	15%		180	210	300	140	290	180	200	250
pH	std. unit	multi-meter		0.1 std. unit	0.05 std. unit		7.5	7.8	7.5	7.6	7.3	7.7	7.5	7.1
DO	(mg/L)	multi-meter		1.5 mg/L	1.0 mg/L		8.6	10	7.9	9.1	4.6	7.4	6.6	9.7
ORP	(mV)	multi-meter		25%	15%		36	10	94	-4.7	-13	25	-4	96
Spec. Cond	(µS/cm)	multi-meter		15%	5%		910	1200	760	480	930	740	660	730
Charge balance	(% differnce)	MINTEQ						8.1	4.1	4.5	7.6	4.1	6	8

Uncertainty (+/- 1σ) associated with isotopic data generated by TI-MS analysis is less than 0.18% for all $^{234}U/^{238}U$ samples and less than 0.0007% for all $^{87}Sr/^{86}Sr$ samples.

Analytical instruments/methods used include: (TI-MS) multi-collector thermal ionization mass spectrometry, (ICP-MS) inductively coupled plasma mass spectrometry, (IC) ion chromatography, (multi-meter) handheld field water chemistry meter, and (field kit) colormetric alkalinity kit.

APPENDIX C

Complete Geochemical Data for Solid Extraction Experiments

Complete Geochemical Data for Solid Extraction Experiments (page 1)

analytical instrument	detection limit	instrument accuracy (+/-)	instrument precision (+/-)	blank
TIMS	ppm	10	10	0
ICP-MS	ppm	10	10	0

Complete Geochemical Data for Solid Extraction Experiments (page 2)

	1/1									1/2									1/3									1/4									1/5									2/1							
	water	(+/-)	acetic	(+/-)	hydrox	(+/-)	total	water	(+/-)	acetic	(+/-)	hydrox	(+/-)	total	water	(+/-)	acetic	(+/-)	hydrox	(+/-)	total	water	(+/-)	acetic	(+/-)	hydrox	(+/-)	total	water	(+/-)	acetic	(+/-)	hydrox	(+/-)	total	water	(+/-)	acetic	(+/-)	hydrox	(+/-)	total	water	(+/-)	acetic	(+/-)	hydrox	(+/-)	total	water	(+/-)	acetic	(+/-)	hydrox	(+/-)	total
$^{234}U/^{238}U$	446							447							542							641							711							712							811							812						
$^{230}Th/^{234}U$	1.29							1.34							1.21							1.20							1.09							1.25							1.17							1.25						
$^{232}Th/^{234}U$	0.0000599	5.0	0.7066	1.0	0.0000601	5.0	0.7066	1.14	2.2%	0.0000605	5.0	0.7066	1.20	15,000	0.70047	1.2%	0.0000667	5.0	0.7080	1.20	15,000	0.70067	1.2%	0.0000627	5.0	0.7080	1.20	15,000	0.70067	1.2%	0.0000630	5.0	0.70481	1.2%	34,000	0.0000596	5.0	0.70747	1.2%	49,000	0.0000667	5.0	0.7088	1.2%	48,000	0.0000668	5.0	0.70839	1.2%	48,000	0.0000639	2.400	0.0000668	2.400	0.70839	2.850	0.3%	11,200
$^{232}Th/^{238}U$	1.09							1.19							1.09							1.20							1.17							1.25							1.17							1.22						
^{232}Th	0.785	1.0	1.30	6.5%	1.30	1.0%	0.479	1.19	0.4%	1.19	2.1%	1.19	0.0%	0.479	3.722	1.6%	1.26	2.1%	25,000	1.29	6.16	30.6%	1.14	1.26	2.1%	25,000	1.29	6.16	30.6%	1.14	46.2	0.7%	1.15	1.2%	247,000	1.09	1.2%	486	0.96	545	1.2%	7,500	2.42	1.7%	1.01	0.0%	592	1.1%	7,530	1.17	39.8	3.2%	1.22	870	4.0%	766	1.9%	12,400
Na	5.410	0.7%	11.8	0.7%	70.7	6.6%	90.5	75.7	1.2%	62.7%	99	1.3%	310,000	16.9	1.0%	14,700	865	1.5%	70.8	3.8%	250,000	73.3	1.5%	1.2%	0.5%	0.7%	64.9	1.0%	1.6%	0.7%	0.7%	1.5%	423,000	0.7%	1.5%	1.0%	20.4%	0.7%	1.5%	1.0%	1.8%	12.0%	37.5	0.7%	72.6	0.9%	30.5	5.1%	51.0	1.0%	948	1.3%	360,000
Mg	4.47	10.6%	1.9	1.2%	5.7	3.9%	12.1	1.86	0.5%	1.91	1.1%	7.0	0.8%	1,800	19.6	1.6%	4.9	2.1%	31.8	2.6%	13.4%	41.0	1.4%	2.4	1.0%	84.6	1.8%	8.6%	601	54.5	1.1%	3.0%	1.2%	35,000	1.1%	1.2%	1.2%	2.0%	30.0	1.8%	0.7%	413	1.2%	1.2%	1.0%	400	1.1%	19.3	16.8	0.3%	372	1.0%	400	1.1%	220	0.1%	828	1.1%	23,100
Si	14.5	5.3%	50.0	2.0%	1.8	4.0%	4.35	15.3	1.1%	16.2	1.7%	4.0	0.0%	15,100	29.6	1.0%	2.0	1.0%	21.0	2.2%	22.4%	28.0	0.9%	1.2%	1.6%	5.1%	8.8	1.2%	1.0%	1.6%	10.3	1.0%	2.0%	0.0%	1.4%	5.7	0.0%	1.2%	1.4%	1.7%	0.0%	321,000	42.1	15.3%	384	15.0%	9.7	0.0%	22.8	2.2%	200	2.6%	534	0.4%	800	1.0%	74,500
K	11.7	2.1%	18.0	3.6%	169	2.6%	6.7%	1.4	2.3%	1.6	1.4%	2.9%	2.9%	2.9%	1.2	1.2%	1.2	1.2%	3.2	1.2%	5.0%	270	1.5%	0.7%	1.6	1.7%	3.6%	3.0%	0.7%	1.1	1.4%	1.2%	1.2%	1.2%	1.2%	1.2%	1.4%	1.4%	1.6%	1.6%	2.7%	524	1.8	3.1%	3.6%	1.6%	28.7	8.4%	239	0.9%	102	0.1%							
Ca	10.2	5.1%	7.8%	2.3%	2.5%	1.0%	0.033	1.7	0.5%	2.5	0.9%	6.6	3.4%	2.3%	14.6	1.9%	1.3	2.2%	3.4	1.2%	82.3%	7.50	1.8%	1.3%	13.9%	605	2.8	0.2%	3.4%	5.4%	6.5	1.8%	1.3%	2.8%	1.2%	1.2%	1.2%	1.2%	1.2%	1.2%	1.2%	19.0	109	0.8%	2,900	1.7%	3,300	0.3%	61.9	24.8%	1,210	13.6%	1,680	1.1%	710	1.2%	304
Sr	9.6	15.1%	10.3%	9.0%	72.1	3.0%	0.033	76.0	1.2%	24.5	0.0%	78.0	1.3%	11,100	1.274	1.6%	1.3	0.3%	1.4	1.2%	7.6%	0.64	1.2%	1.3%	7.6%	799	0.03	0.0%	2.8%	5.6%	0.6	16.1%	3.0%	1.6%	1.2%	1.2%	1.2%	1.2%	1.2%	1.2%	1.2%	6.0	70.3	0.7%	48.6%	2.7%	27,200	0.3%	48.0	0.5%	1,152	1.5%	1,200	1.2%	0.0	0.0	0.0%	0.0%	0.0%	0.0%	0.0%	221	5.5%	671
Ba	0.109	10.7%	68.7	1.1%	71.9	0.8%	1,320	0.197	10.8%	60.9	4.5%	63.4	4.0%	667	0.149	11.9%	9.24	0.9%	11.0	6.3%	1,840	0.667	2.2%	59.4	4.0%	22.0	1.5%	93.4	0.135	2.1%	54.7	0.5%	1.24	4.6%	732	0.052	18.0%	12.3	1.1%	10.9	0.5%	0.232	0.292	0.3%	11.5	1.2%	14.6	0.0%	0.312	23.6%	8.36	6.6%	11.2	0.6%	287	5.8%	4.17
U	0.007	10.3%	16.2	0.4%	24.2	0.0%	0.041	0.0	0.0%	0.0	0.0%	0.0	0.0%	2.1	0.0	0.0%	0.0	0.0%	0.0	0.0%	14.9%	0.0	0.0%	0.0	0.0%	0.0	0.0%	0.0%	0.0	0.0%	0.0	0.0%	0.0%	0.0%	0.0	0.0	0.0%	0.0	0.0%	0.0%	0.0%	0.0	0.0	0.0%	0.0	0.0%	0.0	0.0%	0.0	0.0%	0.0	0.0%	0.0	0.0%	0.0	0.0%	0.0
Mn	1.33	11.2%	66.3	0.0%	0.0	0.0%	0.0	1.8	0.0%	0.0	0.0%	0.0	0.0%	0.0	1.0	1.2%	4.6	0.0%	11.4	1.3%	5.8%	0.0	0.0%	0.0%	0.0%	0.0	0.0%	0.0%	0.0	0.0%	0.0	0.0%	0.0%	0.0%	0.0	0.0	0.0%	0.0	0.0%	0.0%	0.0%	0.0	84.4	11.2%	7.8%	1.2%	0.0	0.0%	0.0	0.0%	0.0	0.0%	0.0	0.0%	0.0	0.0%	0.0
Fe	0.056	0.0%	18.4%	0.4%	0.0	0.0%	0.0	0.0	0.0%	0.0	0.0%	0.0	0.0%	0.0	1.6	0.0%	3.9	0.0%	0.0	0.0%	14.1%	0.0	0.0%	0.0%	0.0%	0.0	0.0%	0.0%	0.0	0.0%	0.0	0.0%	0.0%	0.0%	0.0	0.0	0.0%	0.0	0.0%	0.0%	0.0%	0.0	0.0	0.0%	0.0	0.0%	0.0	0.0%	0.0	0.0%	0.0	0.0%	0.0	0.0%	0.0	0.0%	0.0
Al	0.013	14.9%	12.7%	0.2%	0.0	0.0%	0.0	1.1	0.0%	0.0	0.0%	0.0	0.0%	0.0	1.6	0.0%	3.9	0.0%	0.0	0.0%	14.1%	0.0	0.0%	0.0%	0.0%	0.0	0.0%	0.0%	0.0	0.0%	0.0	0.0%	0.0%	0.0%	0.0	0.0	0.0%	0.0	0.0%	0.0%	0.0%	0.0	0.0	0.0%	0.0	0.0%	0.0	0.0%	0.0	0.0%	0.0	0.0%	0.0	0.0%	0.0	0.0%	0.0
Cu	0.037	6.7%	29.2%	0.4%	0.0	0.0%	0.0	0.0	0.0%	0.0	0.0%	0.0	0.0%	0.0	0.0	0.0%	0.0	0.0%	0.0	0.0%	0.0%	0.0	0.0%	0.0%	0.0%	0.0	0.0%	0.0%	0.0	0.0%	0.0	0.0%	0.0%	0.0%	0.0	0.0	0.0%	0.0	0.0%	0.0%	0.0%	0.0	0.0	0.0%	0.0	0.0%	0.0	0.0%	0.0	0.0%	0.0	0.0%	0.0	0.0%	0.0	0.0%	0.0
Zn	0.047	12.8%	20.4%	0.6%	0.0	0.0%	0.0	0.0	0.0%	0.0	0.0%	0.0	0.0%	0.0	0.0	0.0%	0.0	0.0%	0.0	0.0%	0.0%	0.0	0.0%	0.0%	0.0%	0.0	0.0%	0.0%	0.0	0.0%	0.0	0.0%	0.0%	0.0%	0.0	0.0	0.0%	0.0	0.0%	0.0%	0.0%	0.0	0.0	0.0%	0.0	0.0%	0.0	0.0%	0.0	0.0%	0.0	0.0%	0.0	0.0%	0.0	0.0%	0.0
Pb	0.017	30.1%	23.6%	1.0%	0.0	0.0%	1.7	0.0	0.0%	0.0	0.0%	0.0	0.0%	0.0	0.0	0.0%	0.0	0.0%	0.0	0.0%	0.0%	0.0	0.0%	0.0%	0.0%	0.0	0.0%	0.0%	0.0	0.0%	0.0	0.0%	0.0%	0.0%	0.0	0.0	0.0%	0.0	0.0%	0.0%	0.0%	0.0	0.0	0.0%	0.0	0.0%	0.0	0.0%	0.0	0.0%	0.0	0.0%	0.0	0.0%	0.0	0.0%	0.0
Cd	0.003	14.6%	11.8%	0.0%	0.0	0.0%	1.8	0.2	0.0%	0.0	0.0%	0.0	0.0%	0.0	0.0	0.0%	0.0	0.0%	0.0	0.0%	0.0%	0.0	0.0%	0.0%	0.0%	0.0	0.0%	0.0%	0.0	0.0%	0.0	0.0%	0.0%	0.0%	0.0	0.0	0.0%	0.0	0.0%	0.0%	0.0%	0.0	0.0	0.0%	0.0	0.0%	0.0	0.0%	0.0	0.0%	0.0	0.0%	0.0	0.0%	0.0	0.0%	0.0
Ag	0.0	0.0%	0.0	0.0%	0.0	0.0%	0.0	0.0	0.0%	0.0	0.0%	0.0	0.0%	0.0	0.0	0.0%	0.0	0.0%	0.0	0.0%	0.0%	0.0	0.0%	0.0%	0.0%	0.0	0.0%	0.0%	0.0	0.0%	0.0	0.0%	0.0%	0.0%	0.0	0.0	0.0%	0.0	0.0%	0.0%	0.0%	0.0	0.0	0.0%	0.0	0.0%	0.0	0.0%	0.0	0.0%	0.0	0.0%	0.0	0.0%	0.0	0.0%	0.0
Cr	21.4	10.4%	18.9%	92.4%	0.0	0.0%	9.6	3.1	0.0%	0.0	0.0%	0.0	0.0%	0.0	31.0	0.0%	1.0	0.0%	0.0	0.0%	0.0%	0.0	0.0%	0.0%	0.0%	0.0	0.0%	0.0%	0.0	0.0%	0.0	0.0%	0.0%	0.0%	0.0	0.0	0.0%	0.0	0.0%	0.0%	0.0%	0.0	0.0	0.0%	0.0	0.0%	0.0	0.0%	0.0	0.0%	0.0	0.0%	0.0	0.0%	0.0	0.0%	0.0
P	1.4	3.5%	5.0	15.6%	6.2	2.3%	7.8	2.5	8.7%	3.8	3.1%	2.5	8.7%	1.9	0.9%	3.0	7.5	13.4%	2.1	5.1	69.7%	4.1	2.1	5.1%	4.1	1.9	6.2%	1.9	2.5	1.6	1.9	1.7%	1.6%	1.9%	8.3	0.9	12.2%	2.1%	2.0%	2.1%	0.2%	1.9	0.9	22.1%	5.3	9.9%	2.9	0.2%	0.0	1.8%	4.6	5.9%	2.7	0.6%	0.0	0.0%	0.0
Al	0.057	5.7%	21.0%	0.3%	9.3	2.6%	8.8	19.6	4.5%	15	4.4%	46.0	0.0%	1.7	0.7	0.3%	1.7	1.2%	7.6	1.2%	11.4%	0.7	1.2%	1.7%	0.3%	427	1.2	1.7%	1.2%	1.2%	1.2	1.2%	1.4%	1.2%	1.2	1.4	1.2%	1.2%	1.2%	1.2%	1.2%	0.886	0.057	7.0%	0.557	19.2%	0.947	2.8%	0.009	21.0%	0.508	92.3%	0.729	2.5%							
P	10.2	7.4%	313	7.4%	1,000	30.7%	2,570	2.09	2.3%	41.0	6.7%	212	3.9%	668	1.01	22.5%	46.7	35.9%	154	1.0%	484	2.67	1.6%	49.0	14.8%	253	0.8%	500	1.85	4.5%	243	4.1%	36.5	7.2%	34.2	8.40	34.8%	24.5	14.4%	51.7	17.8%	195																	
As	0.128	3.6%	1.39	26.2%	3.51	5.4%	4.61	1.8%	0.108	1.4%	0.204	86.9%	0.273	3.9%	0.052	4.3%	3.80	6.2%	0.799	0.9%	1.04	37.6%	0.537	36.5%	0.252	18.4%																																

Uncertainties (+/- 1σ) associated with water extraction data are derived by TIMS analysis (less than 1% for $^{234}U/^{238}U$ and $^{230}Th/^{234}U$ ratios; 1-3% for $^{232}Th/^{234}U$ and $^{232}Th/^{238}U$ ratios). Uncertainties for other elements are 1-5% for ICP-MS analysis of acetic, hydrox, and total extractions and 5-10% for ICP-MS analysis of water extractions.

Analytical instruments/methods used include: (TIMS) multi-collector thermal ionization mass spectrometry, (ICP-MS) inductively coupled plasma mass spectrometry.